© 2019. Published by The Company of Biologists Ltd | Journal of Cell Science (2019) 132, jcs235366. doi:10.1242/jcs.235366

RESEARCH ARTICLE

Tetraspanin CD151 and integrin α3β1 contribute to the stabilization of integrin α6β4-containing cell-matrix adhesions

Lisa te Molder, Juri Juksar*, Rolf Harkes, Wei Wang, Maaike Kreft and Arnoud Sonnenberg‡

ABSTRACT

Tetraspanin CD151 has been suggested to regulate cell adhesion through its association with laminin-binding integrins α3β1 and α6β4; however, its precise function in keratinocyte adhesion remains elusive. In this study, we investigated the role of CD151 in the formation and maintenance of laminin-associated adhesions. We show that CD151, through binding to integrin α3β1, plays a critical role in the stabilization of an adhesion structure with a distinct molecular composition of hemidesmosomes with tetraspanin features. These hybrid cell-matrix adhesions, which are formed early during cell adhesion and spreading and at later stages of cell spreading, are present in the central region of the cells. They contain the CD151–α3β1/α6β4 integrin complexes and the cytoskeletal linker protein plectin, but are not anchored to the keratin filaments. In contrast, hemidesmosomes, keratin filament-associated adhesions that contain integrin α6β4, plectin, BP180 (encoded by *COL17A1*) and BP230 (encoded by *DST*), do not require CD151 for their formation or maintenance. These findings provide new insights into the dynamic and complex regulation of adhesion structures in keratinocytes and the pathogenic mechanisms underlying skin blistering diseases caused by mutations in the gene for CD151.

KEY WORDS: Hemidesmosome, Tetraspanin, CD151, Integrin, Plectin, Keratinocyte adhesion

INTRODUCTION

The skin is our largest organ and its barrier function protects us from dehydration and pathogenic infections. To exert these functions, the skin needs to maintain its integrity, for which stable adhesion of basal keratinocytes to the underlying extracellular basal lamina is of paramount importance. This adhesion is largely mediated by hemidesmosomes (HDs), multi-protein complexes that are associated with the keratin intermediate filament system within the cell.

The integrin α6β4, a heterodimeric transmembrane protein, is a main component of HDs. In type I HDs, present in the epidermis, integrin α6β4 binds extracellularly to laminin-332 and intracellularly via two associated proteins, plectin and BP230 (BPAG1e, encoded by *DST*), to the keratin cytoskeleton. Besides integrin α6β4, type I HDs contain two other transmembrane proteins: the tetraspanin CD151 and BP180 (BPAG2 or collagen XVII, encoded by *COL17A1*) (Litjens et al., 2006; Sterk et al., 2000; Walko et al., 2015). In more simple epithelia of the intestine or the mammary gland, a rudimentary form of HDs is present. These type II HDs contain integrin α6β4 and plectin, but lack BP180 and BP230 (Fontao et al., 1997; Uematsu et al., 1994).

In humans, the importance of type I HDs for maintaining skin integrity is underscored by genetic evidence that demonstrates that mutations in any of the six genes encoding HD proteins cause the congenital inherited skin blistering disorder epidermolysis bullosa (EB) (Has and Fischer, 2018). Patients carrying null mutations in the genes for the integrin α6 or β4 subunits, or the cytolinker protein plectin, suffer from a severe form of EB, which is indicated by the absence of HDs (Ashton et al., 2001; McLean et al., 1996; Nakamura et al., 2005; Niessen et al., 1996; Vidal et al., 1995). However, HDs with grossly normal HD structures, but reduced keratin filament association, are found in patients carrying mutations in the genes for BP180 or BP230, and accordingly, these patients only suffer from a mild form of EB (Groves et al., 2010; Jonkman et al., 1995; Liu et al., 2012; McMillan et al., 1998). Mutations in CD151 have not been associated with abnormalities in HDs but nevertheless cause a mild regional skin blistering phenotype, similar to that observed in patients with mutations in the gene encoding integrin α3 (Crew et al., 2004; Has et al., 2012; Kagan et al., 1988; Vahidnezhad et al., 2017). Targeted deletion of genes encoding HDs and associated proteins in mice largely recapitulates the pathology observed in humans (Andrä et al., 1997; DiPersio et al., 1997; Dowling et al., 1996; Guo et al., 1995; Sachs et al., 2006; van der Neut et al., 1996; Wright et al., 2004).

Integrin α3β1, another laminin-binding integrin expressed by keratinocytes, is a component of focal adhesions (FAs), but can also be found together with integrin α6β4 in tetraspanin-enriched microdomains (TEMs) (also named tetraspanin webs). TEMs are formed by lateral associations of tetraspanins with one another and with other proteins. Incorporation of integrins α6β4 and α3β1 in TEMs is facilitated through binding of their α subunits to CD151 (Hemler, 2005). The association of CD151 with laminin-binding integrins has been reported to affect integrin-dependent adhesion, migration and signaling (Berditchevski, 2001; Stipp, 2010; Termini and Gillette, 2017).

While it has been shown that CD151 is colocalized with integrin α6β4 in type I HDs, the exact function of CD151 in the formation of these adhesions or other cell-matrix adhesions in keratinocytes is not known (Sterk et al., 2002). In this study, we assessed the contribution of CD151 to the formation and maintenance of laminin-associated adhesion complexes in keratinocytes. In agreement with data obtained from CD151 knockout mice and patients with *CD151* mutations, our findings confirm that CD151 is not critical for the formation of type I HDs. However, we show that CD151 is essential for the maintenance of adhesion complexes in which CD151 is present together with integrin α3β1 and the HD proteins integrin α6β4 and plectin, but which are not associated with the keratin cytoskeleton.

Division of Cell Biology I, The Netherlands Cancer Institute, Plesmanlaan 121, Amsterdam 1066 CX, The Netherlands.
*Present address Hubrecht Institute, Utrecht, Uppsalalaan 8, Utrecht 3584 CT, The Netherlands.

‡Author for correspondence (a.sonnenberg@nki.nl)

A.S., 0000-0001-9585-468X

Received 14 June 2019; Accepted 28 August 2019

Journal of Cell Science (2019) 132, jcs235366. doi:10.1242/jcs.235366

RESULTS

CD151 forms multi-protein complexes with both integrins α3β1 and α6β4 in keratinocytes

Previous studies have shown that CD151 forms stable complexes with the laminin-binding integrins α3β1 and α6β4 (Hemler, 2005; Sterk et al., 2002). We confirmed these findings by reciprocal co-immunoprecipitation (co-IP) assays using two different monoclonal antibodies against CD151 (5C11 and 11G5) and antibodies against the integrin α3 and α6 subunits (Fig. 1A). Furthermore, these assays showed that in PA-JEB/β4 keratinocytes (immortalized keratinocytes isolated from a patient with pyloric atresia associated with junctional epidermolysis bullosa, and stably expressing wild-type integrin β4) the α6 subunit does not form a heterodimer with β1, which is consistent with the fact that integrins α3β1 and α6β4, but not α6β1, are the major laminin-binding integrins in skin (Sonnenberg et al., 1991) (Fig. 1A). Using immunofluorescence (IF) microscopy, we detected CD151 in a pattern of consecutive arches, in which it is partially co-localized with integrin α3β1. Both integrin α3β1 and CD151 are also found at the cell periphery where they do not colocalize and are present in distinctive adhesion structures (Fig. 1B). Furthermore, both integrin α3β1 and CD151 co-localized with the HD proteins integrin α6β4 and plectin (Fig. 1C,D). In summary, these results confirm that in keratinocytes CD151 binds both integrins α3β1 and α6β4, and is present in adhesion structures that contain characteristics of HDs.

CD151 regulates integrin α6β4 distribution

To determine to what extent CD151 impacts integrin α3β1- and α6β4-containing adhesion complexes, we abrogated CD151 protein expression in PA-JEB/β4 and HaCaT keratinocytes using CRISPR-

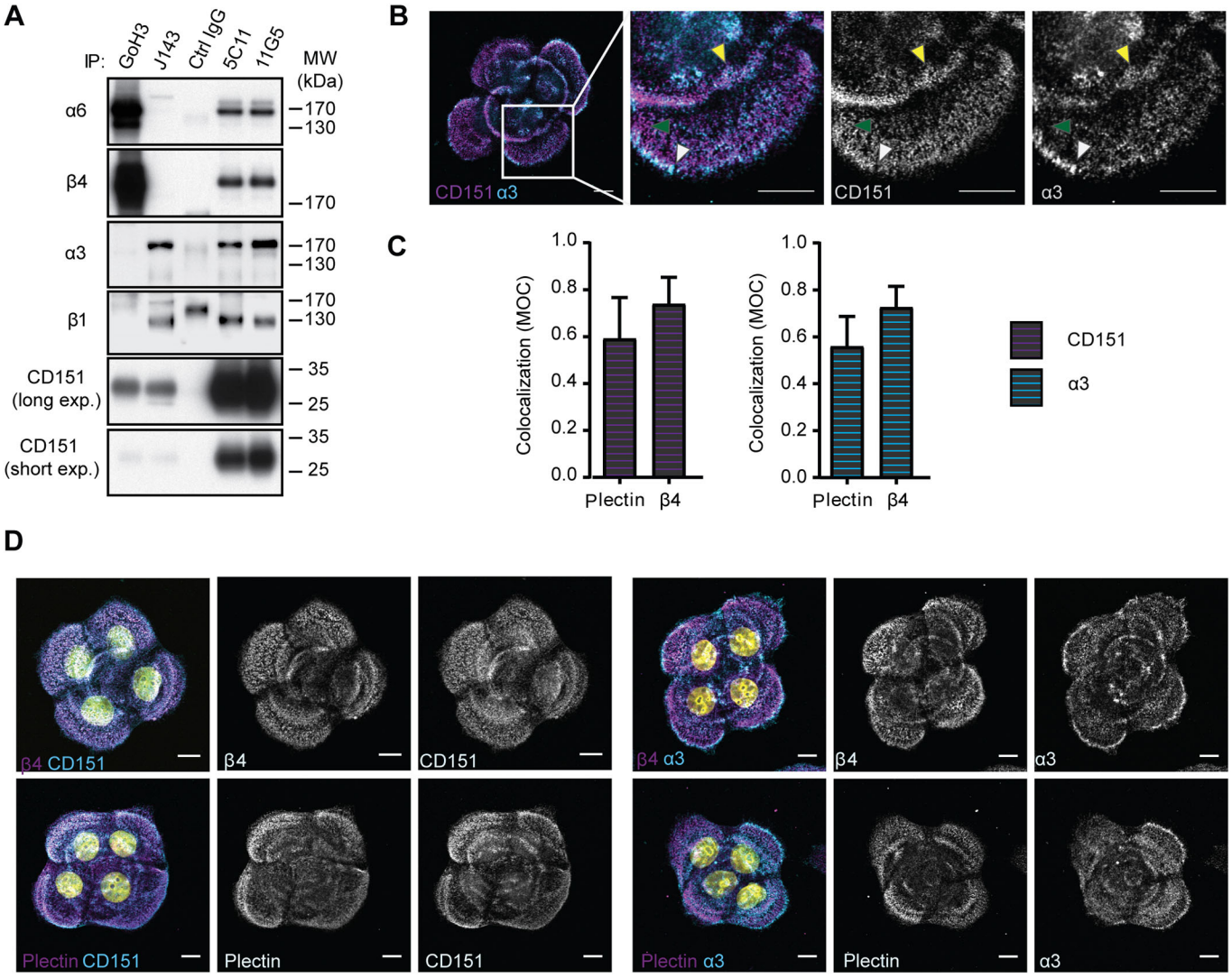

Fig. 1. Association of CD151 with integrins α3β1 and α6β4 in adhesion complexes. (A) Detection of integrin α3β1–CD151 and integrin α6β4–CD151 complexes in lysates of PA-JEB/β4 keratinocytes using immunoprecipitation and western blotting under non-reducing conditions. Antibodies raised against the following proteins were used for immunoprecipitation: GoH3 against integrin α6, J143 against integrin α3, and 5C11 and 11G5 against CD151. (B) Confocal overview and zoom-in image of PA-JEB/β4 cells stained for integrin α3 (cyan) and CD151 (magenta). Yellow arrowheads indicate adhesions containing integrin α3 and CD151 and white and green arrowheads indicate integrin α3 and CD151 located independently of each other in the periphery of the cells. Scale bars: 10 µm. (C) Quantification (mean±s.d.) of the colocalization (Manders' overlap coefficient, MOC) of integrin α3 [46 images from two independent experiments (*N*=2)] or CD151 (30 images; *N*=2) with plectin and integrin α3 (52 images; *N*=2) or CD151 (74 images; *N*=4) with integrin β4. (D) Confocal images of double-IF staining of CD151, integrin α3 (cyan) and HD components plectin and integrin β4 (magenta) in PA-JEB/β4 keratinocytes. Nuclei were counterstained with DAPI (yellow). Scale bars: 10 µm.

Journal of Cell Science (2019) 132, jcs235366. doi:10.1242/jcs.235366

Cas9 (KO) and subsequently restored the expression of CD151 by retroviral-mediated gene transfer. Analysis by western blotting (WB) and fluorescence-activated cell sorting (FACS) confirmed the absence and restoration of CD151 expression, and showed that the deletion of CD151 did not affect the expression of integrins α3β1 and α6β4 at the plasma membrane (Fig. 2A,B). However, quantitative IF staining and confocal microscopy showed reduced clustering of integrin α3β1 (and to a lesser extent of integrin α6β4) at the basal cell surface (Fig. 2C). Furthermore, integrin α3β1 was no longer co-distributed with integrin α6β4 but showed increased co-localization with phospho-paxillin in FAs (Fig. 2D,E). In the CD151-proficient cells, integrin α6β4 was clustered in central and peripheral adhesions, but strikingly in the CD151-deficient cells it was almost exclusively present at the cell periphery (Fig. 2F–H). These results show that, while not essential for integrin α3β1 or α6β4 protein expression or their transport to the plasma membrane, CD151 is necessary for proper organization of these integrins in the central region of the cells.

CD151 is essential for the maintenance of central integrin α6β4-containing adhesions

To gain real-time insight into how CD151 contributes to the formation of integrin α6β4-containing adhesions in the central region of the cells, we deleted CD151 in PA-JEB keratinocytes expressing GFP-tagged integrin subunit β4 (Geuijen and Sonnenberg, 2002). The absence of CD151 and presence of β4–GFP was confirmed by FACS and WB analysis (Fig. 3A,B). The clustering of β4–GFP was followed over time in these cells by time-lapse imaging. During initial stages of cell spreading, both CD151-deficient and -proficient PA-JEB/β4–GFP cells assembled integrin α6β4-containing adhesions at the periphery of the keratinocyte islands. However, while these initial adhesion structures were maintained during later phases of cell spreading and island formation in the CD151-proficient cells, in the CD151-deficient cells, the central adhesion structures resolved and disappeared when the cells formed new peripheral adhesions after cell division and cell spreading (Fig. 3C; Movies 1 and 2). Furthermore, in fluorescence recovery after photobleaching (FRAP) experiments, a spot in the central and peripheral integrin α6β4-containing adhesions was simultaneously bleached and the recovery of the β4–GFP signal at these spots was followed over time (Fig. 3D,E). The results show that the mobile fraction of integrin α6β4 in the central integrin α6β4 adhesions is larger than in the peripheral ones, indicating a higher dynamic nature of integrin α6β4 in the central adhesions (Fig. 3E,F).

Peripheral but not central integrin α6β4-adhesions contain BP230 and are associated with keratin

We reasoned that the observed differences in the dynamics of integrin α6β4 between central and peripheral adhesion clusters could be due to the association of integrin α6β4 with different proteins. Analysis of the distribution of laminin-332 and plectin by total internal reflection fluorescence (TIRF) microscopy showed that both proteins are associated with central and peripheral integrin α6β4-containing adhesions, with laminin-332 being slightly more abundant under the central adhesion clusters and plectin at the peripheral adhesion clusters (Fig. 4A,B). Strikingly, keratin and BP230 (which, like plectin, can connect integrin α6β4 to the keratin cytoskeleton) were associated solely with integrin α6β4 in the peripheral adhesions (Fig. 4A,B). Interestingly, in the peripheral adhesions only approximately 30 and 50 percent of integrin α6β4 was found to be associated with BP230 and keratin, respectively (Fig. 4B). The possibility that the peripheral adhesions lacking keratin and BP230 are associated with the IF protein vimentin can be largely excluded since few PA-JEB/β4 keratinocytes express vimentin and even fewer cells have it associated with peripheral adhesions. For similar reasons, we can exclude that the central adhesions are associated with vimentin (Fig. S1). F-actin, which in many PA-JEB/β4 keratinocytes is organized in a typical circumferential ring, was not obviously associated with either the central or peripheral adhesions (Fig. S1). These results characterize many of the peripheral but not the central integrin α6β4-containing adhesions as type I HDs. Consistent with the notion that type I HDs are present in CD151-deficient patients and mice, the HD proteins BP180, BP230 and plectin were all found to co-localize with integrin α6β4 in the peripheral adhesions of CD151-deficient PA-JEB/β4 keratinocytes (Fig. S2). The central integrin α6β4-containing adhesion clusters, which share some of the characteristics of HDs, such as the clustering of integrin α6β4 and its association with laminin-332 and plectin, also have features in common with TEMs: they contain integrin α3β1 and CD151 and therefore display a hybrid molecular composition. From this point forward, we will refer to these adhesions as central HD-like adhesions in this report.

Integrin α3β1 is localized in central HD-like adhesions but not in peripheral HDs

Despite the fact that CD151 can form stable complex with both integrins α3β1 and α6β4, type I HDs in the skin contain only complexes of CD151 with integrin α6β4 (Sterk et al., 2002; Underwood et al., 2009). To investigate the distribution of integrin α3β1 in relation to CD151 in the different cell-matrix adhesions in the cultured keratinocytes, we performed TIRF imaging and created intensity profiles along a line segment. As shown in Fig. 4, the intensity plots of CD151 and integrin α6β4 in the central HD-like adhesions and the peripheral HDs almost completely overlapped each other (Fig. 4C). In contrast, the profiles of integrins α3β1 and α6β4 only overlapped in the central HD-like adhesions (Fig. 4C). In the peripheral region the peak intensities of integrin α3β1 overlapped with those of tyrosine phosphorylated FA-associated protein paxillin, and not with HD markers BP230 and keratin (Fig. 4D). These results confirm that central and peripheral adhesions differ in protein composition. Furthermore, while in the central HD-like adhesions integrin α3β1, integrin α6β4 and CD151 cluster together, in the periphery they can be found in two distinct complexes: integrin α3β1 in FAs and integrin α6β4 and CD151 in type I HDs.

CD151 stabilizes central HD-like adhesions through binding to integrin α3β1 and self-association

Our findings so far indicate that CD151 is essential for maintaining central HD-like adhesions. To determine whether CD151 stabilizes these adhesions through binding to integrin α3β1, we deleted and reconstituted integrin α3 in the HaCaT and PA-JEB/β4 keratinocyte cell lines (Fig. 5A,B; Fig. S3A,B). In both these cell lines, the absence of integrin α3 did not affect the total levels of integrin β4 at the cell surface and the formation of peripheral HDs was not obviously disturbed. However, as observed in the CD151-deficient PA-JEB/β4 keratinocytes, the absence of integrin α3 caused a loss of central HD-like adhesions, albeit less dramatically (Fig. 5B–D; Fig. S3C). To exclude the possibility that the absence of the central HD-like adhesions is caused by reduced spreading of the integrin α3-deficient cells, we also analyzed the cells that were plated on coverslips coated with a mixture of vitronectin and fibronectin. Under these conditions, cell spreading of the integrin α3-deficient cells was increased and found to be comparable to that of the wild-

Journal of Cell Science (2019) 132, jcs235366. doi:10.1242/jcs.235366

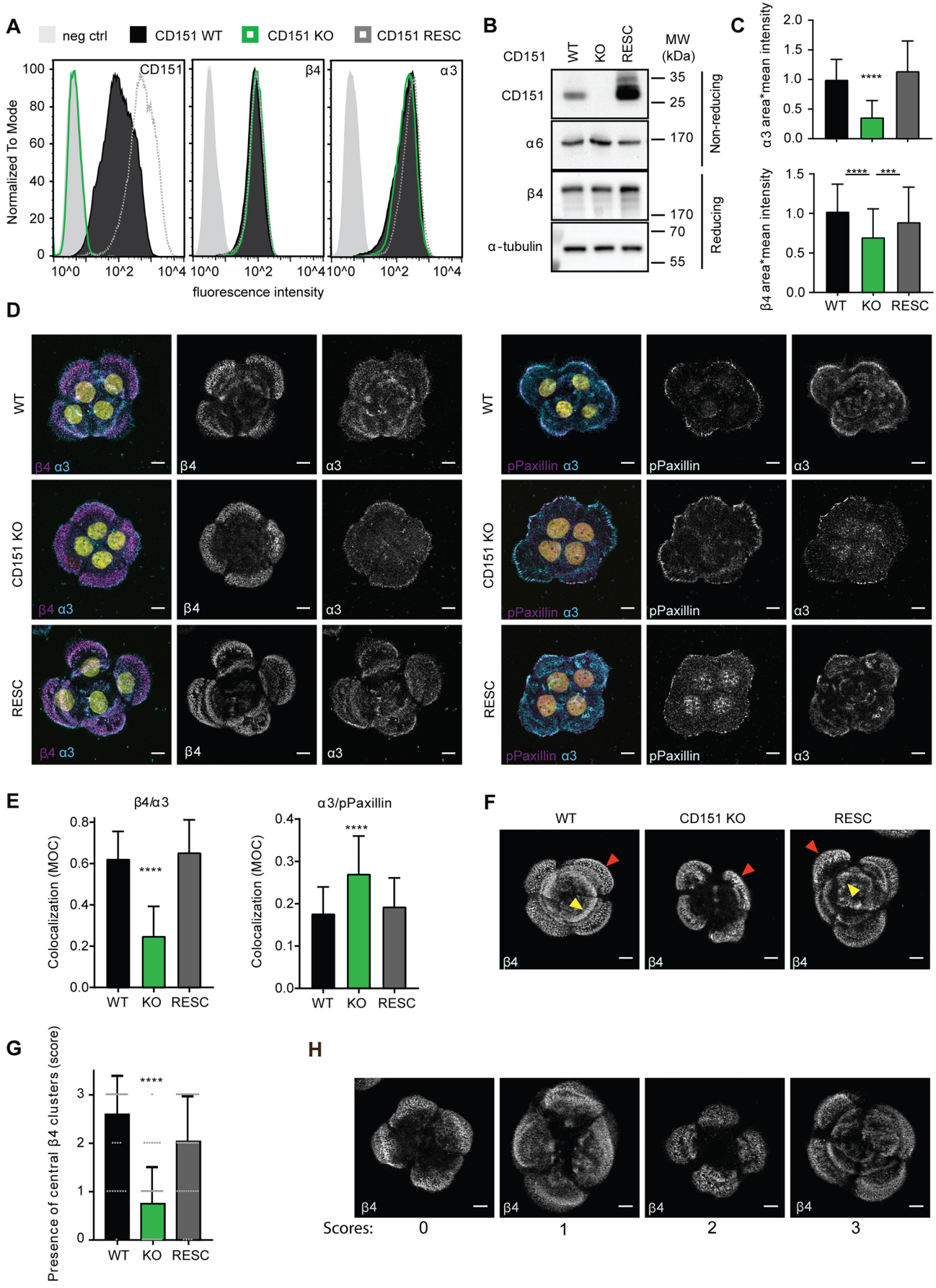

Fig. 2. See next page for legend.

Journal of Cell Science (2019) 132, jcs235366. doi:10.1242/jcs.235366

Fig. 2. CD151 influences localization of adhesions containing integrins α3β1 and α6β4. (A) FACS analysis of surface expression of CD151, integrin β4 and integrin α3 for wild-type (WT), CD151 knockout (CD151-KO) and rescue (CD151-RESC) PA-JEB/β4 cells. (B) Whole-cell lysate of WT, CD151-KO and CD151-RESC PA-JEB/β4 keratinocytes analyzed by western blotting for protein levels of CD151, integrin α6, integrin β4 and α-tubulin (loading control) under reducing or non-reducing conditions as indicated. (C) Quantification (mean±s.d.) of the amount of integrin α3 (WT, 55; KO, 57; RESC, 55 images; *N*=3) and integrin β4 (WT, 122; KO, 122; RESC, 119 images; *N*=8) clustering at the basal cell surface (integrin α3 or integrin β4 area×intensity). ***P<0.001, ****P<0.0001 (Mann–Whitney *U*-test). (D) Confocal images of WT, CD151-KO and CD151-RESC PA-JEB/β4 keratinocytes stained for integrin α3 (cyan) and integrin β4 (magenta), or integrin α3 (cyan) and phosphorylated paxillin (magenta). Nuclei were counterstained with DAPI (yellow). Scale bars: 10 µm. (E) Quantification (mean±s.d.) of the colocalization (MOC) of integrin β4 and integrin α3 (WT, 56; KO, 55; RESC, 57 images; *N*=3) and of integrin α3 and phosphorylated paxillin (WT, 55; KO, 57; RESC, 55 images; *N*=3). ****P<0.0001 (Mann–Whitney *U*-test). (F) Confocal images of WT and CD151-KO and CD151-RESC PA-JEB/β4 keratinocytes stained for integrin β4. Red arrowheads show peripheral integrin α6β4-containing adhesions, while yellow arrowheads point to central integrin α6β4-containing adhesions. Scale bars: 10 µm. (G) Quantification (mean±s.d.) of the amount of central integrin α6β4-containing adhesions per cell island (dots represent individual cell islands) using images from WT (57 images; *N*=4), CD151-KO (56 images; *N*=4) and CD151-RESC (55 images; *N*=4) PA-JEB/β4 cells stained for integrin β4. ****P<0.0001 (Mann–Whitney *U*-test). (H) Scoring system for the amount of central integrin α6β4-containing adhesions present, with example images. 0=no central adhesion, 1=few central adhesions, 2=several central adhesions, 3=many central adhesions. Scale bars: 10 µm.

type cells on uncoated coverslips. Importantly, the difference in the amount of central HD-like adhesions persisted between the integrin α3-deficient and -proficient cells (Fig. S3D,E).

Next, we investigated whether the role of integrin α3β1 in maintaining the central HD-like adhesions requires binding of integrin α3β1 to laminin-332. To this end, we introduced a binding-deficient integrin α3 mutant (G163A) into integrin α3-deficient HaCaT cells (Zhang et al., 1999). Expression of the mutant integrin α3β1 was verified by FACS analysis (Fig. 5B). Unlike the wild-type integrin α3 subunit, the integrin α3-G163A mutant was unable to completely rescue the central HD-like adhesions, suggesting that integrin α3β1 binding to laminin contributes to efficient maintenance of these adhesions (Fig. 5C,D). These findings were confirmed in PA-JEB/β4 cells using the integrin α3 blocking antibody, J143 (Fig. S3F,G).

Palmitoylation of CD151 is necessary for stabilization of the CD151 TEMs and hence for incorporation and clustering of integrins α3β1 and α6β4 into these multi-molecular complexes of CD151 (Berditchevski et al., 2002; Yang et al., 2002). To study the role of this self-associating function of CD151 for stabilization of the central HD-like adhesions, we introduced a CD151 palmitoylation mutant into the CD151-deficient PA-JEB/β4 keratinocytes (Fig. 5B) (Berditchevski et al., 2002). The expression of this mutant in CD151 KO cells did not rescue the central HD-like adhesions, suggesting that for the maintenance of these clusters CD151 needs to form multi-molecular complexes by oligomerization (Fig. 5E,F; Fig. S3H).

Taken together, these results show that for efficient maintenance of the central HD-like adhesions, both laminin-332-associated integrin α3β1 and self-associated and TEM-forming CD151 are needed.

Laminin-332, but not plectin, contributes to clustering of integrin α6β4 in central HD-like adhesions

Since the peripheral HDs and central HD-like adhesions contain more plectin and laminin, respectively, we studied whether CD151-mediated clustering of integrin α6β4 in the different adhesions requires binding of integrin α6β4 to laminin-332 or plectin. Therefore, we expressed the integrin β4 mutants, β4-AD and β4-RW, in integrin β4-deficient PA-JEB keratinocytes (Fig. 6A). The β4-AD mutant is an adhesion-defective mutant that cannot bind to laminin-332, while the β4-RW mutant, carrying a single missense mutation R1281W in the cytoplasmic domain of integrin β4, is unable to bind plectin (Geerts et al., 1999; Nievers et al., 2000; Russell et al., 2003). In the β4-AD mutant-expressing cells, central HD-like adhesions were less commonly present than in the wild-type integrin β4 (β4-WT)-expressing cells (Fig. 6B,C). Similar findings were obtained when PA-JEB/β4 and HaCaT cells were treated with the integrin β4 blocking antibody ASC8 (Russell et al., 2003). In the presence of this blocking antibody, the central HD-like adhesions are mostly absent, while there are abundant peripheral HDs (Fig. 6D,E). In the cells expressing the β4-RW mutant and in plectin-deficient PA-JEB/β4 keratinocytes, the integrin α6β4 staining was diffused and adhesions were less well-defined. Nevertheless, in many cell islands some central HD-like adhesions could be observed (Fig. 6B,C,F,H). In addition, the loss of plectin resulted in a reduction of peripheral HDs (Fig. 6G,H). These results indicate that the binding of integrin α6β4 to laminin-332, as for integrin α3β1, contributes to the stabilization of the central HD-like adhesions. By contrast, binding of integrin α6β4 to plectin is not essential, but might contribute to the clustering of this integrin in the peripheral type I HDs.

CD151 does not affect the strength of integrin α6β4-mediated cell adhesion

Integrin clustering determines the strength with which cells adhere to the extracellular matrix (ECM) (Puklin-Faucher and Sheetz, 2009). To investigate whether CD151-mediated clustering of integrins α3β1 and α6β4 strengthens the adhesion of keratinocytes to laminin-332 deposited by the cells to the substratum, we quantified the adhesion strength of CD151-proficient and -deficient HaCaT keratinocytes, which express both integrin α3β1 and α6β4, using a spinning disk device (Boettiger, 2007). CD151-deficient cells showed a reduced tolerance (albeit not statistically significant) of shear stress compared to the CD151-proficient cells (Fig. 7A), suggesting that CD151 plays only a minor role in adhesion strengthening when both integrins α3β1 and α6β4 are present. Next, we investigated whether cell adhesion mediated by either integrin α3β1 or α6β4 is strengthened by CD151. To resolve this, we individually deleted integrin α3 and integrin β4 in the CD151-deficient HaCaT keratinocytes and confirmed the absence of these proteins by FACS and WB analysis (Fig. 7B,C). The deletion of integrin α3 in the CD151-deficient HaCaT keratinocytes had no effect on the adhesive strength of integrin α6β4 to laminin-332 (Fig. 7D). However, in the absence of integrin α6β4, the additional loss of CD151 resulted in a significant reduction in integrin α3β1-mediated adhesion strengthening (Fig. 7E,F). We conclude that CD151 significantly strengthens integrin α3β1-, but not integrin α6β4-mediated cell adhesion by facilitating the clustering of this integrin into central HD-like adhesions.

DISCUSSION

CD151 has been shown to be broadly expressed by a variety of cell types and to form complexes with different laminin-binding integrins, including integrins α3β1 and α6β4 (Sincock et al., 1997). In skin, CD151 is complexed with integrin α6β4 and is a component of HDs (Sterk et al., 2000). In this study, we show that in cultured keratinocytes CD151 is not only present in HDs, but also in an adhesion structure with a distinct molecular composition of a HD with tetraspanin features. These hybrid adhesion structures, which are present in the central region of the cell, and referred to as central

Journal of Cell Science (2019) 132, jcs235366. doi:10.1242/jcs.235366

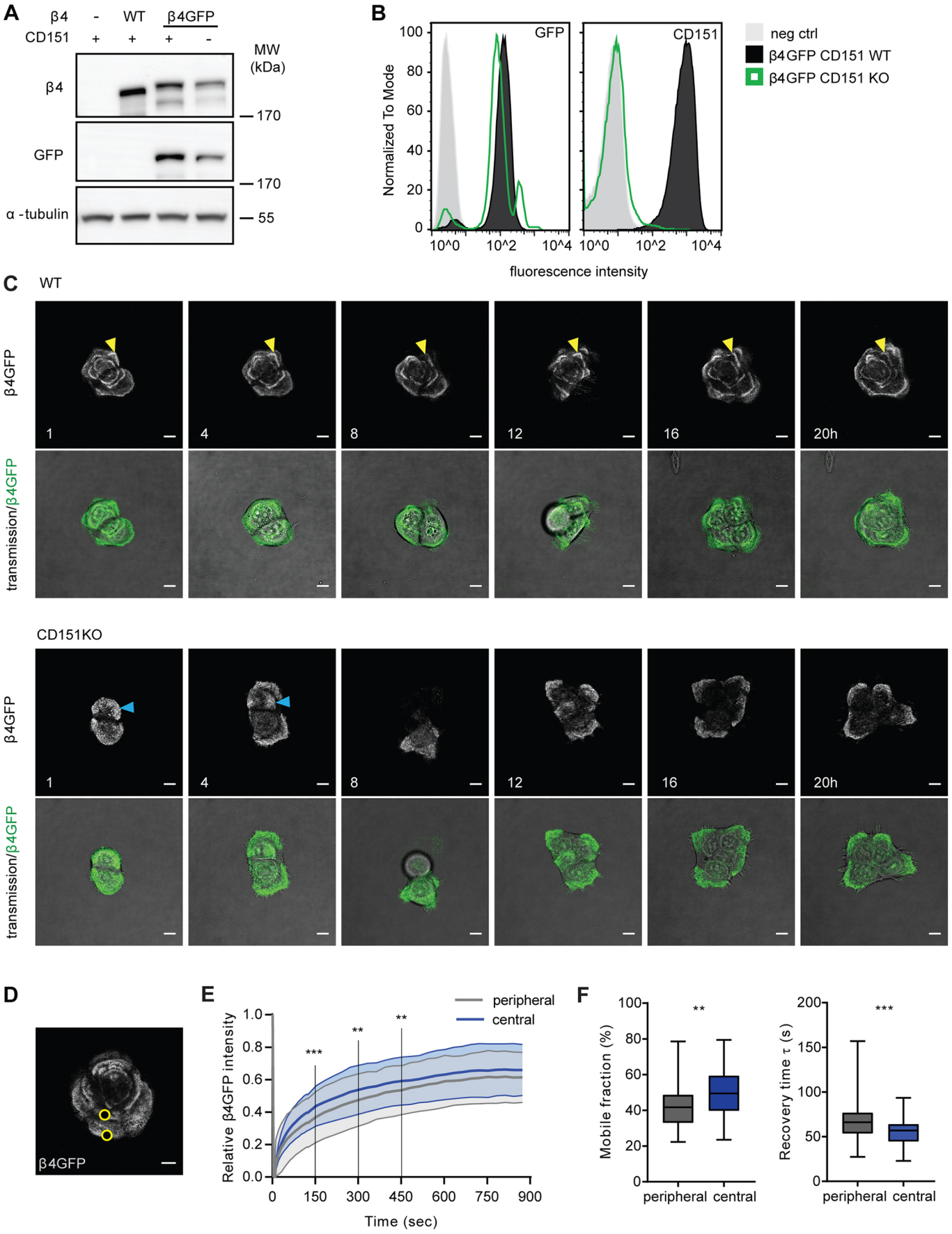

Fig. 3. See next page for legend.

Journal of Cell Science (2019) 132, jcs235366. doi:10.1242/jcs.235366

Fig. 3. CD151 is essential for maintenance of early integrin α6β4-containing adhesions. (A) Western blotting analyses of WT or CD151-KO PA-JEB keratinocytes, reconstituted with WT-β4 or integrin β4–GFP. Whole cell lysates were tested for integrin β4, GFP and α-tubulin protein levels. (B) FACS analyses of CD151 and integrin β4–GFP surface expression on WT and CD151-KO PA-JEB/β4–GFP cells. (C) Stills from a time-lapse experiment using WT and CD151-KO PA-JEB/β4–GFP cells. Top panels show the integrin β4–GFP signal and bottom panels the overlay of the integrin β4–GFP and DIC signal. Stills show images taken at 1, 4, 8, 12, 16 and 20 h after addition of DMEM+FCS (0 h time point, 20 h after seeding). The yellow arrowheads indicate a peripheral adhesion becoming a central adhesion over time in WT cells and the blue arrowheads indicate a peripheral adhesion disappearing over time in KO cells. Scale bars: 10 µm. (D) Example image of PA-JEB/β4–GFP after the bleach step of a FRAP experiment; FRAP regions indicated in peripheral and central adhesions with yellow circles. Scale bar: 10 µm. (E) Integrin β4–GFP intensity (relative to the mean integrin β4–GFP intensity before bleaching) over time (in seconds) during FRAP experiments in both central (blue) and peripheral (grey) integrin α6β4-containing adhesions. Data was collected from 38 islands in three experiments, lineplot shows the mean+s.d. (F) Mobile fraction and recovery time of integrin β4–GFP in central and peripheral adhesions during the first 230 s of the same dataset used for E. Boxplots divide the data in quartiles and the median is indicated. The whiskers show minimal and maximal values. $^{**}P<0.01$, $^{***}P<0.001$ (Wilcoxon matched-pairs signed rank test) in E,F.

HD-like adhesions, contain the cytolinker plectin in addition to the CD151–α3β1/α6β4 integrin complexes, but are not associated with keratin filaments. We further show that CD151, through its binding to integrin α3β1, is critical for the formation and stabilization of these central HD-like adhesions and strengthens integrin α3β1- but not integrin α6β4-mediated keratinocyte adhesion to laminin-332. CD151 is not needed for the formation of type I HDs that are formed in the periphery of the cells and are anchored to keratin filaments (Fig. 8).

The mechanistic reasons for the lack of association of keratin filaments with the central HD-like adhesions can be surmised based on previous studies. PKA-mediated phosphorylation of plectin at S4642 interferes with its interaction with intermediate filaments (Bouameur et al., 2013), and therefore, it is possible that plectin is phosphorylated at this residue in the central HD-like adhesions, which prevents its association with keratin filaments. Additionally, BP230, which is present in peripheral HDs but not central HD-like adhesions, may be required for efficient attachment of keratin filaments to the plasma membrane. In support of this supposition, BP230 knockout mice showed an impaired connection of keratin filaments with HDs (Guo et al., 1995). Similarly, reduced amounts of keratins are associated with type II HDs, which contain plectin but lack BP230 (Fontao et al., 1997; Uematsu et al., 1994).

Although an essential role of CD151 in the formation of type I HDs was not evident from our current experiments, a more subtle role of CD151 for the formation of HDs cannot be excluded. The ability of CD151 to facilitate the clustering of integrins α3β1 and α6β4 into central HD-like adhesions may strengthen keratinocyte adhesion to newly deposited laminin-332 before FAs and HDs are fully established; however, once integrins are connected to the cytoskeleton, the function of CD151 as a clustering molecule may no longer be required. This model would indicate an important role of CD151-mediated adhesion strengthening and clustering of integrins α3β1 and α6β4 into central HD-like adhesions *in vivo*. For example, during re-epithelization of wounded skin, when HDs are dissolved and stable adhesion of the keratinocytes to the basal lamina is no longer assured, the central HD-like adhesions may prevent detachment of migrating keratinocytes that are subject to external mechanical forces. At the same time, they may render the adhesion of keratinocytes sufficiently dynamic to allow integrin turnover and migration to occur. Consistent with a role of the central HD-like adhesions in migration, we found that these adhesions are more dynamic than the type I HDs.

Despite the fact that the association of BP230 with keratin filaments at type I HDs increases their stability (Michael et al., 2014; Seltmann et al., 2013), our FRAP analyses showed only a modest increase in the stability of the peripheral HD adhesions compared to the central HD-like adhesions. Since our FRAP analyses do not distinguish between peripheral adhesions that are or are not associated with keratin filaments, this apparent discrepancy may be explained by the notion that not all of the peripheral adhesions are associated with keratin filaments. Furthermore, it should be understood that the peripheral type I HDs lack integrin α3β1, whose presence in the HD-like adhesions contributes to their stability.

In central HD-like adhesions, CD151 and integrin α3β1 colocalize, but in the periphery CD151 associates with type I HDs and integrin α3β1 is localized into FAs. The localization of integrin α3β1 into FAs coincides with the incorporation of BP230 in HDs. Since the localization of BP180 in type I HDs precedes that of BP230 (Koster et al., 2003), it is possible that BP180 displaces integrin α3β1 from CD151 and allows the integrin to become incorporated into FAs. In this respect it is interesting to mention that, like CD151 and the integrin α3, α6 and β4 subunits (Yang et al., 2004), BP180 contains several cysteine residues adjacent to its transmembrane domain that are potential sites of palmitoylation. The role of protein palmitoylation in the formation of HDs is not known, but it is reasonable to suggest that it might help to increase the local concentration of HD proteins, and facilitate the assembly and stability of HDs.

In agreement with our finding that HDs can be formed in the absence of integrin α3β1 in cultured keratinocytes, no obvious abnormalities in HDs have been observed in mice lacking integrin α3 in basal keratinocytes (Conti et al., 2003; DiPersio et al., 1997; Margadant et al., 2009). Yet, genetic ablation of the β1 integrin subunit or its co-activator kindlin-1 (encoded by *FERMT1*) in basal keratinocytes has been associated with reduced HD protein expression and formation of HDs (Brakebusch et al., 2000; Qu et al., 2012; Raghavan et al., 2000). This suggests that if integrin α3β1 has a role in HD formation, this role could be fulfilled by other integrins, as well. Furthermore, our finding that CD151 contributes to integrin α3β1- but not integrin α6β4-mediated strengthening of cell adhesions is consistent with the respective roles these proteins play in mediating cell-matrix adhesion in the skin and kidney. In the skin, where basal keratinocytes express both integrins α3β1 and α6β4, the effect of CD151 deletion is relatively mild, and patients display only a mild skin blistering disorder. In contrast, the loss of CD151 in glomerular podocytes, which express integrin α3β1 but not integrin α6β4, has been associated with progressive and irreversible kidney dysfunction (Crew et al., 2004; Kagan et al., 1988; Sachs et al., 2012; Vahidnezhad et al., 2017).

In conclusion, we show that CD151 stabilizes the central HD-like adhesions by strengthening the adhesion of integrin α3β1 to laminin-332 and facilitating the incorporation of integrin α6β4 into TEMs containing integrin α3β1. By contrast, CD151 is not needed for the formation or stabilization of integrin α6β4-containing type I HDs in the periphery of the cells, which are linked to keratin filaments. These data provide new insights into the role of CD151 in the formation and maintenance of different populations of adhesions that are formed in cultured keratinocytes. Importantly, our study reflects the skin conditions observed in patients and mice with mutations in CD151 and integrin α3β1, and thus provides better understanding of the mechanisms underlying these conditions.

Journal of Cell Science (2019) 132, jcs235366. doi:10.1242/jcs.235366

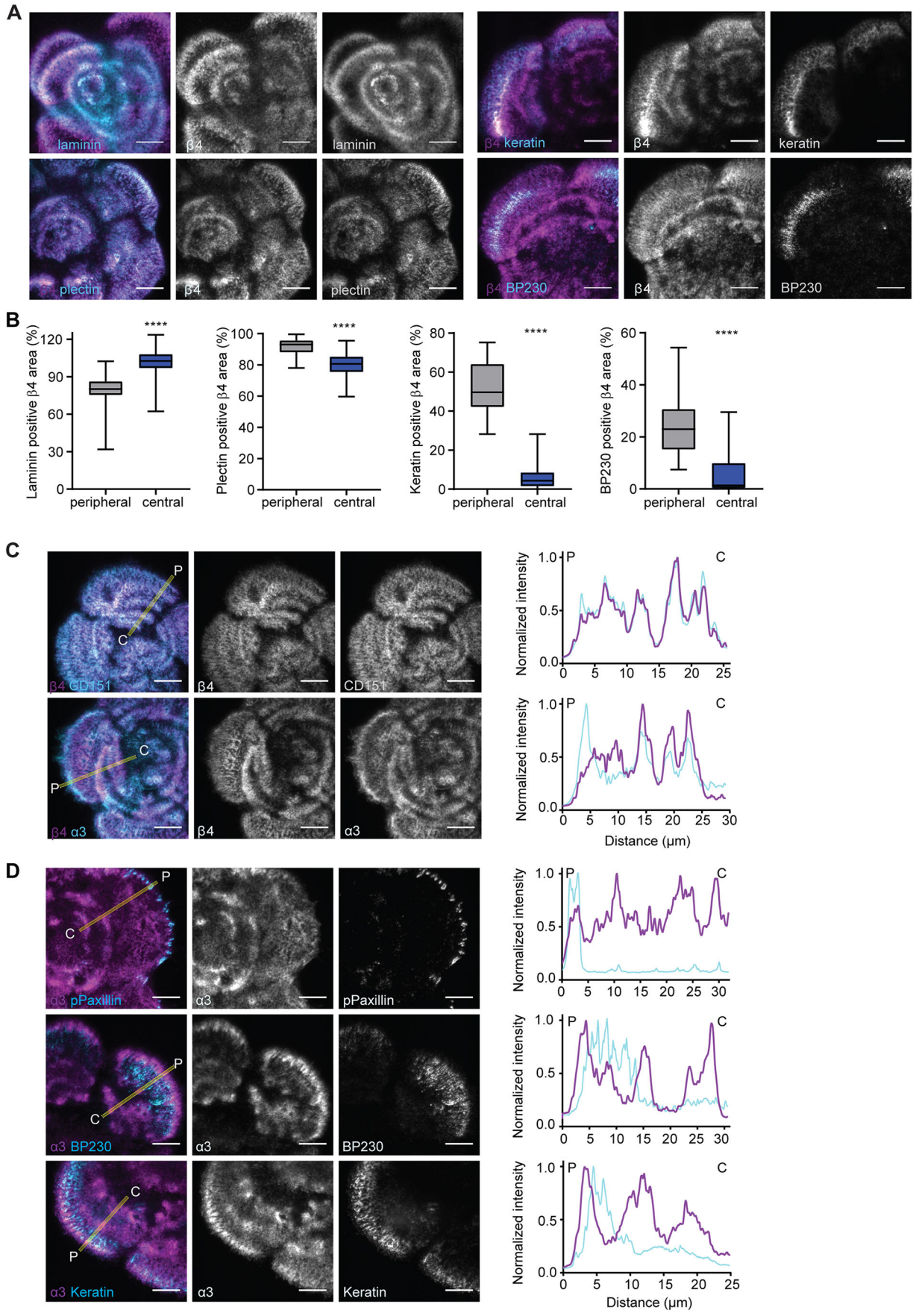

Fig. 4. See next page for legend.

Journal of Cell Science (2019) 132, jcs235366. doi:10.1242/jcs.235366

Fig. 4. Central and peripheral adhesions differ in protein composition. (A) TIRF images of PA-JEB/β4 keratinocytes stained for integrin β4 (magenta) and laminin-332, plectin, keratin-14 or BP230 (cyan). Scale bars: 10 µm. (B) Quantification of the integrin β4 area which is positive for laminin-332 (57 images; *N*=2), plectin (60 images; *N*=2), keratin-14 (59 images; *N*=2) or BP230 (61 images; *N*=2) in peripheral and central integrin α6β4-containing adhesions. Boxplots divide the data in quartiles and the median is indicated. The whiskers show the minimal and maximal values. ****P<0.0001 (Mann–Whitney *U*-test). (C,D) TIRF images of PA-JEB/β4 cells stained for integrin β4 (magenta) and CD151 or integrin α3 (cyan) (C), or integrin α3 (magenta) and phosphorylated paxillin, BP230 or keratin (cyan) (D). Scale bars are 10 µm. Line plot shows the relative fluorescence intensities (normalized to the highest pixel intensity) of the different proteins along the line (thickness: 10 pixels) indicated in the overlay image. The line starts in the periphery (P) and is drawn towards the center (C) of the island.

MATERIAL AND METHODS

Antibodies

The primary and conjugated antibodies used in this study are listed in Table S1. Secondary antibodies for western blotting were goat anti-mouse IgG HRP (1:3000; Bio-Rad, 170-6516) and polyclonal goat anti-Rabbit IgG HRP (1:5000; Dako, P044801-2). Donkey anti-mouse IgG PE (1:500; Jackson ImmunoResearch, 715-116-150) was the secondary antibody used in FACS. For immunofluorescence (IF), rabbit anti-rat IgG (1:1000; in-house), goat anti-guinea pig IgG Alexa Fluor 488, goat anti-human IgG Alexa Fluor 488, goat anti-mouse Alexa Fluor 568, goat anti-mouse Alexa Fluor 647, goat anti-rabbit Alexa Fluor 488, goat anti-rabbit Alexa Fluor 647, goat anti-rat Alexa Fluor 647 (1:200; Invitrogen, A-11073, A-11013, A-11004, A-21236, A-11034, A-21245, A-21247), goat anti-mouse FITC, goat anti-rat FITC (1:200; Rockland, 610-102-121 and 612-102-120) and the isotype-specific goat anti-mouse IgG1 Alexa Fluor 568 (1:500; Thermo Fisher Scientific, A-21124) and goat anti-mouse IgG2a FITC (1:250; Abcam, ab98697) were used secondary antibodies.

Cell lines

PA-JEB immortalized keratinocytes were isolated from a patient with pyloric atresia associated with junctional epidermolysis bullosa (Niessen et al., 1996; Schaapveld et al., 1998). The derivation of this cell line was done for diagnostic purposes, thus, the research conducted using these cells was exempt from the requirement for ethical approval. PA-JEB/β4

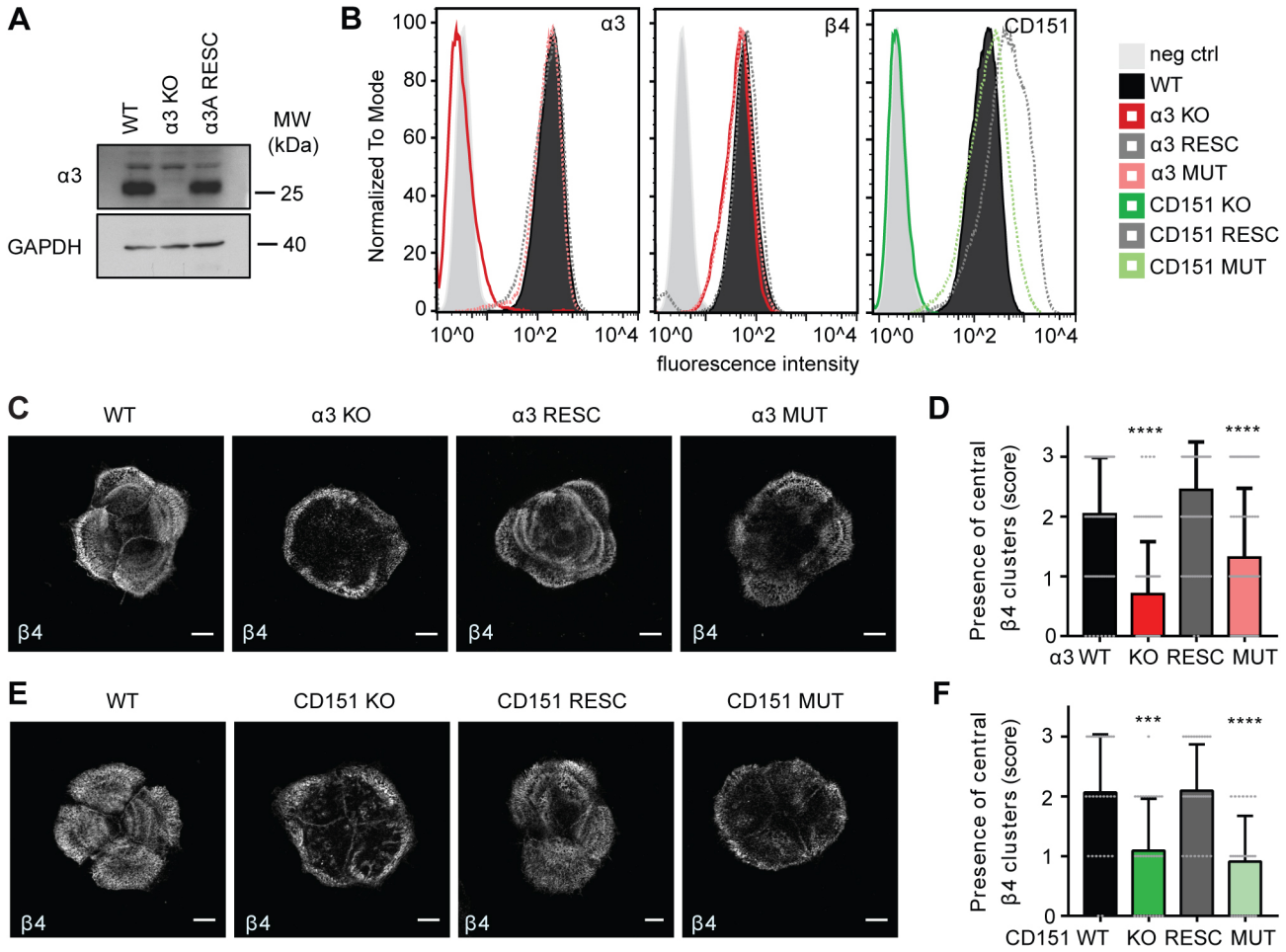

Fig. 5. Integrin α3β1 and CD151-self association contribute to stabilization of central HD-like adhesions. (A) Whole-cell lysate of WT, α3-KO and α3-RESC HaCaT keratinocytes analyzed for protein levels of integrin α3 and GAPDH (loading control) by western blotting. (B) FACS analyses of integrin α3, integrin β4 or CD151 surface expression on WT, α3-KO, α3-RESC, mutated integrin α3 (α3-MUT), CD151-KO, CD151-RESC and CD151-MUT HaCaT keratinocytes. (C) Confocal images of integrin β4 in WT and α3-KO, α3-RESC and α3-MUT HaCaT keratinocytes. Scale bars: 10 µm. (D) Quantification (mean ±s.d.) of the presence of central integrin β4 clusters (score 0–3, dots represent individual score values) in WT (101 islands; *N*=4) and α3-KO (98 islands; *N*=4), α3-RESC (103 islands; *N*=4) and α3-MUT (102 islands; *N*=4) HaCaT keratinocytes. ****P<0.0001 (Mann–Whitney *U*-test). (E) Confocal images of integrin β4 in WT and CD151-KO, CD151-RESC and CD151-MUT HaCaT cells. Scale bars: 10 µm. (F) Quantification (mean±s.d.) of the presence of central integrin β4 clusters (score 0–3) in WT (31 islands; *N*=2) and CD151-KO (33 islands; *N*=2), CD151-RESC (32 islands; *N*=2) and CD151-MUT (33 islands; *N*=2) cells. ***P<0.001, ****P<0.0001 (Mann–Whitney *U*-test).

Journal of Cell Science (2019) 132, jcs235366. doi:10.1242/jcs.235366

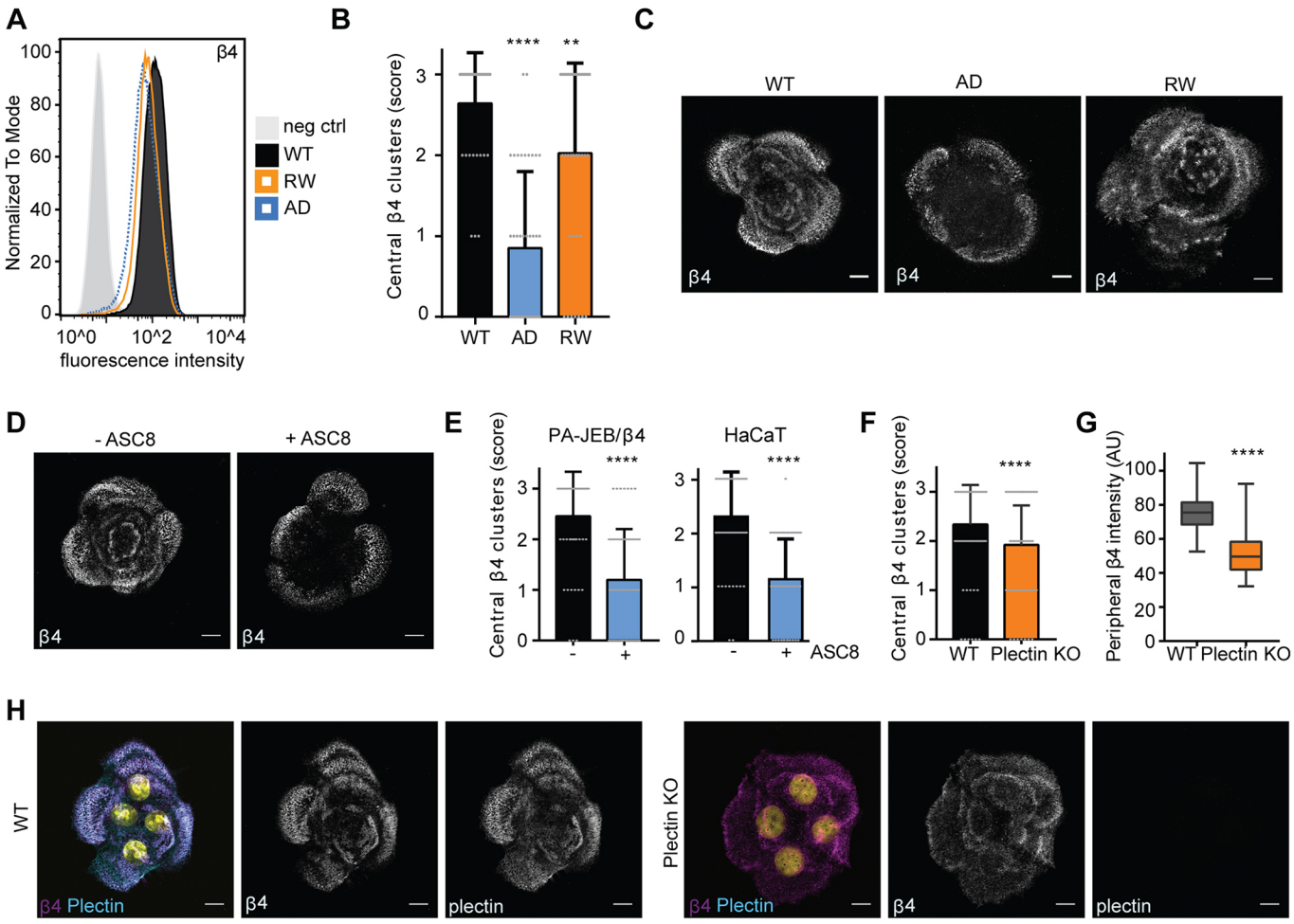

Fig. 6. Laminin but not plectin binding to integrin α6β4 contributes to stabilization of central HD-like adhesions. (A) FACS analyses of integrin β4 surface expression on WT, and β4-AD- and β4-RW-expressing PA-JEB keratinocytes. (B) Quantification (mean±s.d.) of the central integrin β4 clusters (score 0–3, dots represent individual score values) in WT (39 images; *N*=3), β4-AD (40 images; *N*=3) and β4-RW (42 images; *N*=3). ***P*<0.01, *****P*<0.0001 (Mann–Whitney *U*-test). (C) Confocal images of integrin β4 in WT, β4-AD and β4-RW PA-JEB/β4 keratinocytes. Scale bars: 10 µm. (D) Confocal images of integrin β4 in WT PA-JEB/β4 keratinocytes grown on coverslips for 2 days in the absence (–) or presence (+) of integrin β4 blocking antibody ASC8. Scale bars: 10 µm. (E) Quantification (mean±s.d.) of the presence of central integrin β4 clusters (score 0–3) in WT PA-JEB/β4 treated without (59 images; *N*=3) or with (60 images; *N*=3) ASC8, and HaCaT keratinocytes treated without (60 images; *N*=3) or with (60 images; *N*=3) ASC8. *****P*<0.0001 (Mann–Whitney *U*-test). (F) Quantification (mean±s.d.) of the presence of central integrin β4 clusters (score 0–3) in WT (110 images; *N*=6) and plectin-KO (102 images; *N*=6) PA-JEB/β4 keratinocytes. *****P*<0.0001 (Mann–Whitney *U*-test). (G) Quantification of the mean intensity of integrin β4 clustered in the peripheral adhesions in WT (73 images; *N*=4) and plectin-KO (71 images; *N*=4) PA-JEB/β4 cells. Boxplots divide the data in quartiles and the median is indicated. The whiskers show the minimal and maximal values. *****P*<0.0001 (Mann–Whitney *U*-test). (H) Confocal images of integrin β4 (magenta) and plectin (cyan) in WT and plectin-KO PA-JEB/β4 keratinocytes. Scale bars: 10 µm.

keratinocytes stably expressing wild-type β4 were generated by retroviral transduction (Sterk et al., 2000) and maintained in serum-free keratinocyte medium (KGM; Invitrogen), supplemented with 50 µg ml^{-1} bovine pituitary gland extract, 5 ng ml^{-1} EGF, and antibiotics (100 units ml^{-1} streptomycin and 100 units ml^{-1} penicillin; Sigma-Aldrich). Human HaCaT keratinocytes were obtained from Dr Fusenig of the German Cancer Center (DKFZ) in Heidelberg, Germany and cultured in Dulbecco's modified Eagle's medium (DMEM; Gibco) containing 10% heat-inactivated fetal calf serum (FCS; Serana) and antibiotics. All cells were cultured at 37°C in a humidified, 5% CO_2 atmosphere.

The integrin α3-, integrin β4-, CD151- and plectin-deficient cells were prepared using CRISPR-Cas9 technology. Target sgRNAs against integrin α3 (5′-GCTACTCGGTCGCCCTCCAT-3′), integrin β4 (5′-GACTCGCT-CCCTCCGCGCCT-3′), CD151 (5′-CAGGTTCCGACGCTCCTTGA-3′) and plectin (5′-GAGGTGCTTGTTGACCCACT-3′) were cloned into the pX330-U6-Chimeric_BB-CBh-hSpCas9 (Addgene plasmid #42230, deposited by Feng Zhang). For the integrin α3-, integrin β4- and CD151-deficient cells, cells were transiently transfected with this plasmid using Lipofectamine® 2000 (Invitrogen) in OptiMEM (Gibco). The cells were bulk sorted for the population deficient of the protein of interest using a Moflo Asterios (Beckman Coulter) or FACSAria Fusion (BD Biosciences) cell sorter. For the preparation of the plectin-deficient cells, cells were co-transfected with a plasmid containing a blasticidin cassette flanked by TIA target sites (described by Blomen et al., 2015), blasticidin-resistant cells were enriched by selection for four days in the presence of blasticidin (4 µg ml^{-1}; Sigma-Aldrich), clones were picked and analyzed for plectin expression by western blotting.

For (re)expression of proteins in protein-deficient cells, we used stable cellular retroviral-mediated transduction. Cells that expressed the protein were enriched by zeocin or blasticidin selection and/or by bulk sorting by FACS. The constructs used were: the β4-AD mutant (D230A, P232A and E233A) in LZRS-IRES-blasticidin, a kind gift from Peter Marinkovich (Russell et al., 2003), the CD151 wild-type and CD151 palmitoylation mutant in LZRS-IRES-Zeo, constructed by introducing the CD151 cDNA released from pZeo-CD151 or pZeo-CD151-PALM [gift from F. Berditchevski (Berditchevski et al., 2002)] and the integrin α3 wild-type

Journal of Cell Science (2019) 132, jcs235366. doi:10.1242/jcs.235366

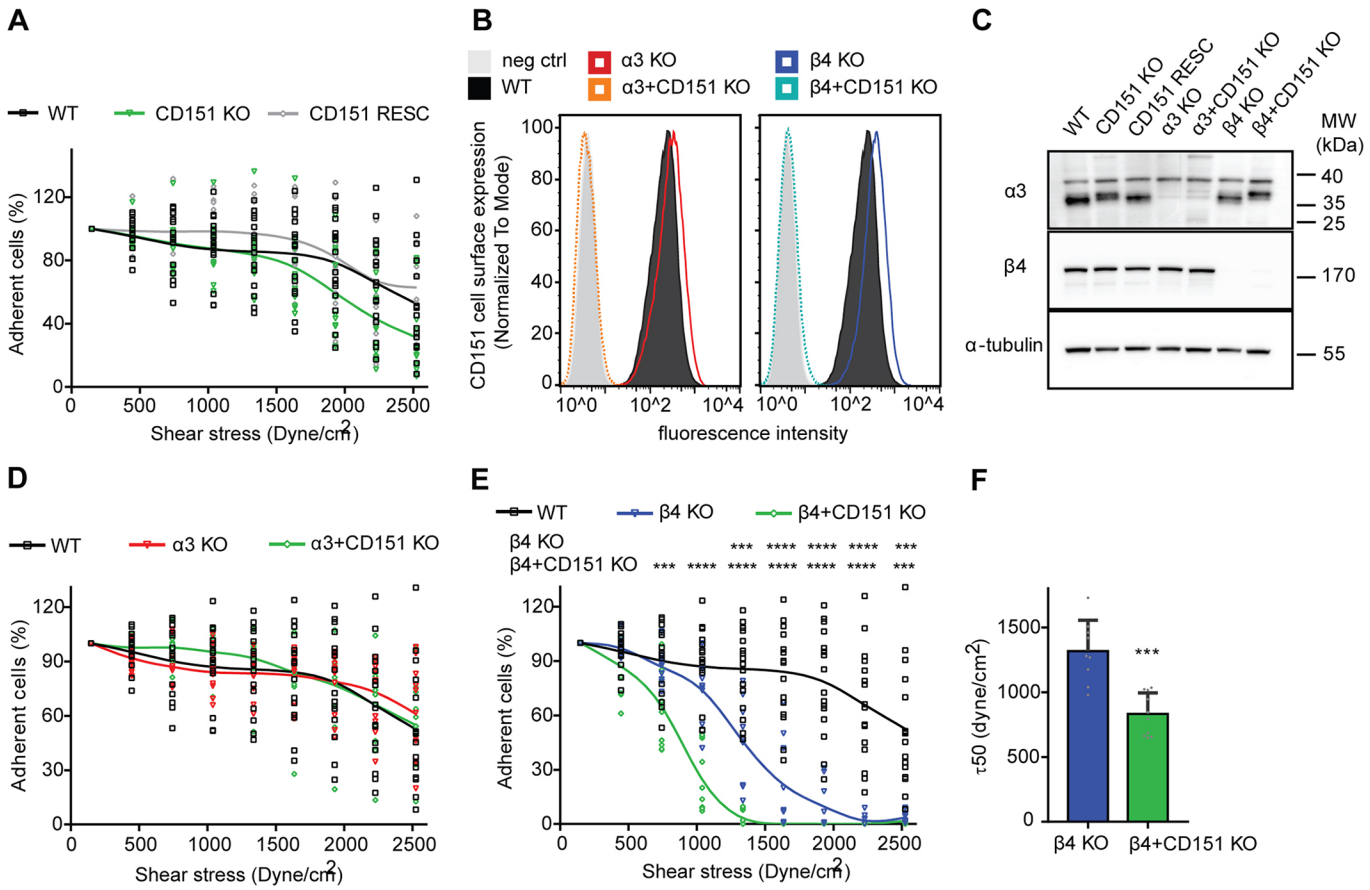

Fig. 7. CD151 contributes to integrin α3β1-mediated adhesion strengthening. (A) Percentage of WT (squares; *n*=16), CD151-KO (triangles; *n*=13) and CD151-RESC (diamonds; *n*=14) HaCaT keratinocytes that remained adherent under conditions of increasing shear stresses (shown in dynes/cm^2). Line depicts the mean; no significant differences detected (unpaired *t*-tests corrected for multiple comparisons). (B) CD151 surface expression of WT, α3-KO, β4-KO and double α3+CD151 and β4+CD151 KO HaCaT keratinocytes analyzed by FACS. (C) Expression of integrin α3, integrin β4 and α-tubulin (loading control) in whole-cell lysates from WT, CD151-KO and CD151-RESC, α3-KO, β4-KO and double α3+CD151 and β4+CD151 KO HaCaT keratinocytes analyzed by western blotting. (D,E) Percentage of WT (squares; *n*=16), α3-KO (triangles; *n*=11) and double α3+CD151 KO (diamonds; *n*=11) HaCaT keratinocytes (D) and of WT (squares; *n*=16), β4-KO (triangles; *n*=9) and double β4+CD151 KO (diamonds; *n*=10) HaCaT keratinocytes (E) that remained adherent after being submitted to increasing conditions of shear stresses (in dynes/cm^2). Line depicts the mean; ***P<0.001, ****P<0.0001 (unpaired *t*-tests corrected for multiple comparisons). (F) Mean±s.d. τ50 calculated for β4-KO and double β4+CD151 KO HaCaT cells from the same dataset shown in E. ***P<0.001 (Mann–Whitney *U*-test).

in LZRS-IRES-Zeo. The integrin α3 cDNA has been described previously (Delwel et al., 1994) and the full-length cDNA encoding human integrin α3 was released from pUC18 by digesting with *Sph*I, made blunt by Klenow digestion and ligated into the *Swa*I site of the retroviral LZRS-IRES-zeo vector. Furthermore, the integrin α3-G163A mutant in pBJ-1 expression vector (Zhang et al., 1999) was a gift from Yoshikazu Takada (University of California, Davis, USA) and transiently transfected in α3-deficient cells. Generation of PA-JEB keratinocytes stably expressing integrin β4 [β4RW (R1281W)] has been described previously (Geerts et al., 1999).

Immunofluorescence imaging of fixed samples

For image acquisition, cells were seeded at ∼10–20% confluence onto glass coverslips, uncoated or coated with 10 µg ml^{-1} fibronectin from bovine plasma (F1141, Sigma-Aldrich) and 5 µg ml^{-1} vitronectin (SRP3186, Sigma-Aldrich) and grown for 40–44 h of which at least the last 20 h in the presence of DMEM+FCS. After the cells had been fixed with 2% PFA for 10 min, permeabilized with 0.2% Triton X-100 and blocked with 2% BSA (resolved in PBS; Serva), they were incubated for 50–60 min with primary and secondary antibodies, with three PBS washes in between. Nuclei were counterstained with DAPI (Sigma-Aldrich) and coverslips were mounted with MOWIOL for confocal imaging. For TIRF imaging, coverslips were stored in PBS at 4°C until imaging.

Confocal imaging was performed using a Leica TCS SP5 confocal microscope with a 63× (NA 1.4) oil objective. A Leica SR-GSD microscope (Leica Microsystems, Wetzlar, Germany) equipped with a 160× oil immersion objective (NA 1.47) and an EMCCD Andor iXon camera (Andor Technology, Belfast, UK) was used to acquire TIRF images with an imaging depth of 200 nm. To be able to perform subsequent analyses, imaging was performed under consistent conditions.

Image analyses were performed using ImageJ: Co-localization was assessed using Manders' overlap coefficient (MOC) with the JACoP plugin. The amount of basal cell surface clustering was quantified by calculating the integrated density of the staining. The intensity of the integrin β4 staining in the peripheral adhesions was obtained by drawing a region of interest around the peripheral adhesions and measuring the mean intensity of the integrin β4 staining in this region. The percentage of integrin β4 associated with plectin, BP230, keratin 14 or laminin-332 was obtained by calculating how much of the integrin β4-positive area was additionally positive for plectin, BP230, keratin or laminin-332. The quantification of the island sizes was performed by thresholding images based on their staining with Phalloidin-iFluor647 (AAT Bioquest) and measuring the surface area after selecting the outer region. Furthermore, the quantification of the amount of central integrin β4 clusters present per cell island was performed using an arbitrary scoring system (0=no central adhesions, 1=few central adhesions, 2=several central adhesions, 3=many central adhesions).

Journal of Cell Science (2019) 132, jcs235366. doi:10.1242/jcs.235366

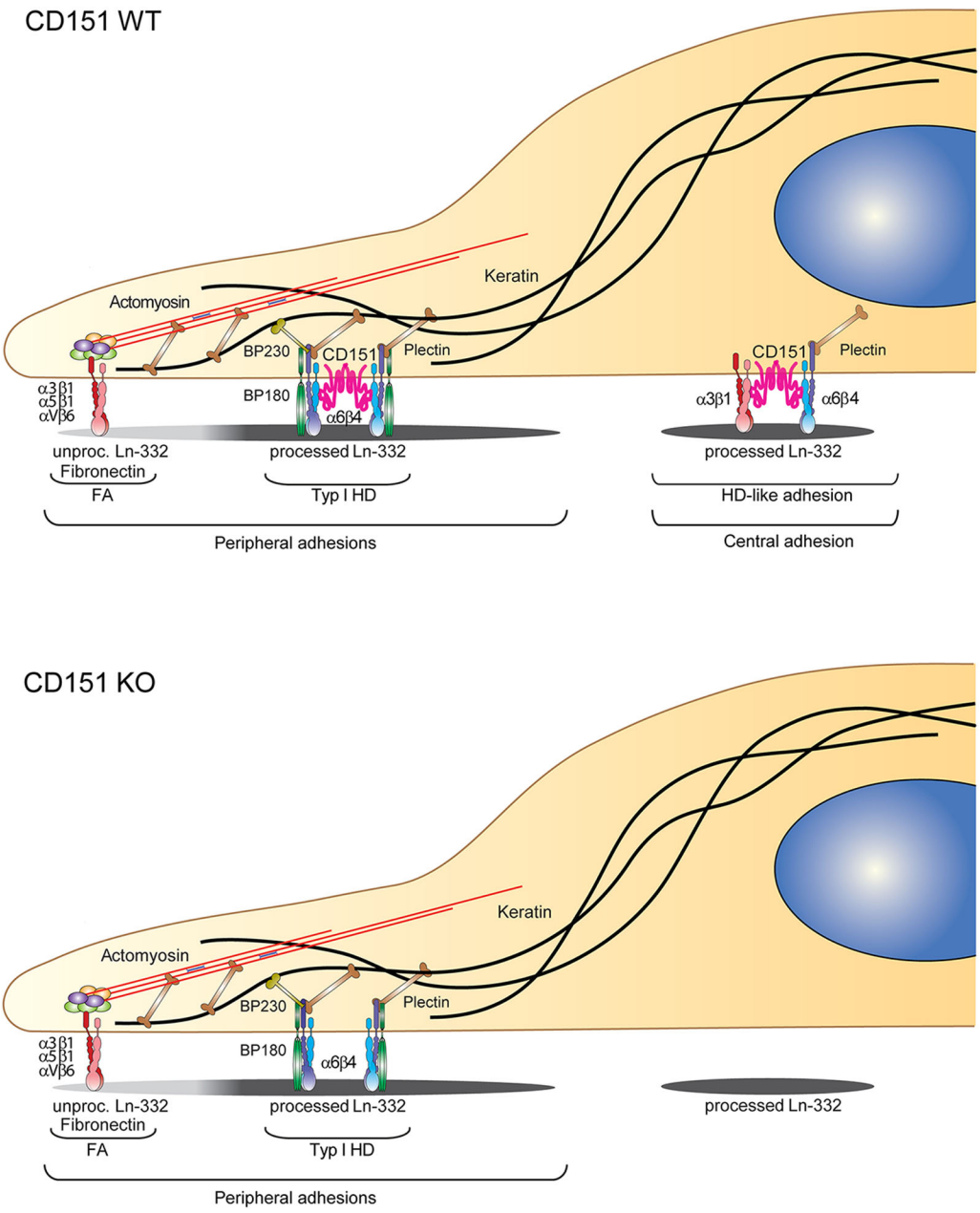

Fig. 8. CD151 is essential for the maintenance of central HD-like adhesions but not the formation of peripheral FAs and type I HDs. In the presence of CD151 (top panel), integrins α3β1 and α6β4 are present together with CD151 in central HD-like adhesions. Additionally, integrin α3β1 is present in FAs in the periphery of the cell island preceding the type I HDs in which integrin α6β4 is present also together with CD151. In the absence of CD151 (bottom panel), the peripheral adhesions are still formed but lack CD151, while the central HD-like adhesions are lost.

Graphs were made using GraphPad Prism and include bar graphs showing the mean±s.d. (including dots that represent independent measurement) or boxplots dividing the data in quartiles. The number of images used for analyses is specified in the figure legends and statistical significance was calculated using the non-parametric and non-paired Mann–Whitney *U*-test; *P*-values: *<0.05, **<0.01, ***<0.001, ****<0.0001.

Live imaging and FRAP

For live imaging and fluorescence recovery after photobleaching (FRAP), cells were seeded on 24 mm coverslips and imaging was performed using a Leica TCS SP5 confocal microscope with a 63× (NA 1.4) oil objective equipped with a live cell chamber. Live imaging of CD151-proficient and -deficient PA-JEB/β4–GFP cells was started 20 h after seeding and immediately after replacing the KGM medium with DMEM+FCS. Every hour the differential interference contrast (DIC) and GFP fluorescence signals were collected from multiple cell islands at different positions. Videos were made in ImageJ.

FRAP experiments were performed, using the FRAP wizard in LAS-AF (Leica), using PA-JEB/β4–GFP cells grown for 20 h in KGM medium and subsequently grown for an additional 20 h in DMEM+FCS. Simultaneously, a region in one peripheral and one central integrin α6β4-containing adhesion was bleached and fluorescent recovery was followed over time. Two images as controls were taken before bleaching and then one image every 10 s (first 2 min) or 30 s for 15 min after bleaching. For analyses, the background was subtracted from the measured intensities and the curves were normalized to the mean value before bleaching. Furthermore, the values of the first 230 s were fitted with a single exponential decay using MATLAB software and the fitted curve was used to calculate the mobile fraction and the recovery time τ. Graphs were made using GraphPad Prism; the line plot shows the mean±s.d. and the boxplots divide the data in quartiles. The number of images used for analyses is specified in the figure legends and the significance difference between the central and peripheral adhesions was calculated using the non-parametric Wilcoxon matched-pairs signed rank test (at different time points); *P*-values: **<0.01, ***<0.001.

Flow cytometry and FACS

For FACS analyses, cells were collected after trypsinization, and incubated for 50–60 min with primary and secondary antibodies on ice in PBS

containing 2% FCS. In between the antibody steps, cells were washed twice with 2% FCS in PBS. Finally, cells were passed through a nylon mesh filter and 50000+ cells were analyzed per sample using a FACSCalibur cell analyzer (BD Biosciences). Cells incubated with only secondary antibody were used as a negative control. Graphs include values of a representative experiment (out of three repetitions) normalized to the mode. The graphs were made in FlowJo and adapted in Adobe Illustrator.

Adhesion strengthening assay

To measure long-term adhesion strength of cells, we used the spinning disk assay described by Boettiger (2007). Wild-type or KO HaCaT cells were grown to 60–100% confluence on 30 mm coverslips for 2 days. Just before spinning, the cells were washed briefly with PBS and the coverslips were 'glued' to the stamp using grease. The cells were spun for 8 min at 4240 rpm in PBS-ABC buffer [80% A (10 gl^{-1} NaCl, 0.25 gl^{-1} KCl, 0.95 gl^{-1} Na_2HPO_4*$2H_2$, 0.25 gl^{-1} KH_2PO_4), 10% B (1.34 gl^{-1} $CaCl_2.2H_2O$) and 10% C (2 gl^{-1} $MgCl_2.6H_2O$)] containing 5% dextran from *Leuconostoc* spp. M_r 450,000–600,000 (Sigma-Aldrich). After spinning, the cells were fixed in 2% PFA, permeabilized in 0.2% Triton X-100, stained with DAPI and mounted on microscopic slides using MOWIOL. The complete coverslips were imaged using a Zeiss AxioObserver Z1. The coverslip area was divided in rings with a 1.5 mm diameter and the cell confluence was measured per ring and normalized to the total area of the ring and to the confluence in the middle area (100% confluent). The average shear stress per ring was calculated using the formula $\tau = 10 \times \left(0,8\ r\ \sqrt{\rho\mu\omega^3}\right)$ with τ is the shear stress in dynes/cm^2, r is the radial distance from the center of rotation in m, ρ is the fluid density in kg m^{-3}, μ is the fluid viscosity in Pa s and ω is the rotational velocity in radians min^{-1}. The $\tau 50$ was obtained by fitting the data points to a logistic function $f = \frac{100}{1+\exp[(\tau - c)/b]}$ using MATLAB software, where c is the inflection point and equal to the point of 50% cell detachment ($\tau 50$) and b is the slope at the inflection point.

Graphs were generated and significance was calculated using GraphPad Prism. The line plots show the mean value of the 9–16 experiments per condition, which are individually shown as squares, diamonds or triangles. For the wild-type line, the same dataset was used in the different graphs. The significance of the percentage of adherent cells in KO cells compared to the wild-type cells was calculated at each data point using unpaired *t*-tests corrected for multiple comparisons using the Holm–Sidak method; *P*-values: ***<0.001, ****<0.0001. The $\tau 50$ was visualized in a bar graph showing the mean±s.d. of 9–10 independent experiments. The significant different between the $\tau 50$ in integrin β4 KO and integrin β4+CD151 KO cells was calculated using the non-parametric Mann–Whitney *U*-test; *P*-value: ****<0.0001.

Immunoprecipitations and western blotting

For analysis of proteins in whole cell lysates, sub-confluent cells were washed in cold PBS, lysed in RIPA (1% NP-40, 0.5% sodium deoxycholate, 0.1% SDS, 4 mM EDTA pH 7.5, 100 mM NaCl, 20 mM Tris-HCl pH 7.5) supplemented with inhibitors (1.5 mM Na_3VO_4, 15 mM NaF and 1:500 protease inhibitor cocktail), whole-cell lysates were cleared by centrifugation at 15,000 ***g*** for 60 min at 4°C and supplemented with SDS sample buffer (50 mM Tris-HCl pH 6.8, 2% SDS, 10% glycerol, 12.5 mM EDTA, 0.02% Bromophenol Blue) with or without β-mercaptoethanol and heated at 95°C for 5 min. Immunoprecipitations were performed with cell lysates prepared in 1% NonidetP-40, 100 mM NaCl, 4 mM EDTA, 20 mM Tris-HCl (pH 7.5), supplemented with inhibitors. After centrifugation at 15,000 ***g*** for 60 min at 4°C, the cleared lysates were incubated at 4°C for 1.5 h with 1 µg ml^{-1} antibody. Subsequently, the lysates were incubated overnight with Protein G Sepharose 4 Fast Flow beads (GE Healthcare), beads were washed three times with lysis buffer and two times with PBS and bound proteins were dissolved in SDS sample buffer without β-mercaptoethanol and heated at 95°C for 5 min.

Proteins were separated on 4–12% bolt Novex gradient gels (Invitrogen) and transferred to Immobilon-P transfer membranes (Millipore). The membrane was blocked for at least 2.5 h in 2% BSA in TBST (10 mM Tris pH 7.5, 150 mM NaCl, 0.05% Tween 20) before incubation with primary antibody overnight at 4°C and with secondary antibody for 1 h at room temperature. After each incubation, membranes were washed twice with TBST and twice with TBS (TBST without Tween 20). Antibodies were detected using Clarity Western ECL Substrate (Bio-Rad) and in the figures the molecular mass markers (kDa) are indicated.

Acknowledgements

We thank Leila Nahidiazar, Bram van den Broek, Lenny Brocks and Marjolijn Mertz for their help with imaging and image analysis; Martijn van Baalen, Anita Pfauth, Frank van Diepen and Debajit Bhowmick for their help with cell sorting; Alba Zuidema, Veronika Ramovs, Jose de Pereda and Kevin Wilhelmsen for critical reading of the manuscript. Furthermore, we thank our colleagues for sharing reagents.

Competing interests

The authors declare no competing or financial interests.

Author contributions

Conceptualization: L.t.M., A.S.; Methodology: L.t.M., J.J., W.W., M.K.; Software: R.H.; Validation: L.t.M.; Formal analysis: L.t.M.; Investigation: L.t.M., J.J.; Writing - original draft: L.t.M., A.S.; Writing - review & editing: L.t.M., R.H., W.W., A.S.; Visualization: L.t.M.; Supervision: A.S.

Funding

This work was supported by grants from the Nederlandse Organisatie voor Wetenschappelijk Onderzoek (Netherlands Organization for Scientific Research, NWO; project number 824.14.010), the KWF Kankerbestrijding (Dutch Cancer Society; project number 2013-5971) and by a grant from NWO as part of the National Roadmap Large-scale Research Facilities of the Netherlands, Proteins@Work (project number 184.032.201).

Supplementary information

Supplementary information available online at
http://jcs.biologists.org/lookup/doi/10.1242/jcs.235366.supplemental

References

Andrä, K., Lassmann, H., Bittner, R., Shorny, S., Fässler, R., Propst, F. and Wiche, G. (1997). Targeted inactivation of plectin reveals essential function in maintaining the integrity of skin, muscle, and heart cytoarchitecture. *Genes Dev.* **11**, 3143-3156. doi:10.1101/gad.11.23.3143

Ashton, G. H., Sorelli, P., Mellerio, J. E., Keane, F. M., Eady, R. A. J. and McGrath, J. A. (2001). Alpha 6 beta 4 integrin abnormalities in junctional epidermolysis bullosa with pyloric atresia. *Br. J. Dermatol.* **144**, 408-414. doi:10.1046/j.1365-2133.2001.04038.x

Berditchevski, F. (2001). Complexes of tetraspanins with integrins: more than meets the eye. *J. Cell Sci.* **114**, 4143-4151.

Berditchevski, F., Odintsova, E., Sawada, S. and Gilbert, E. (2002). Expression of the palmitoylation-deficient CD151 weakens the association of alpha 3 beta 1 integrin with the tetraspanin-enriched microdomains and affects integrin-dependent signaling. *J. Biol. Chem.* **277**, 36991-37000. doi:10.1074/jbc.M205265200

Blomen, V. A., Májek, P., Jae, L. T., Bigenzahn, J. W., Nieuwenhuis, J., Staring, J., Sacco, R., van Diemen, F. R., Olk, N., Stukalov, A. et al. (2015). Gene essentiality and synthetic lethality in haploid human cells. *Science* **350**, 1092-1096. doi:10.1126/science.aac7557

Boettiger, D. (2007). Quantitative measurements of integrin-mediated adhesion to extracellular matrix. *Meth. Enzymol.* **426**, 1-25. doi:10.1016/S0076-6879(07)26001-X

Bouameur, J.-E., Schneider, Y., Begré, N., Hobbs, R. P., Lingasamy, P., Fontao, L., Green, K. J., Favre, B. and Borradori, L. (2013). Phosphorylation of serine 4,642 in the C-terminus of plectin by MNK2 and PKA modulates its interaction with intermediate filaments. *J. Cell Sci.* **126**, 4195-4207. doi:10.1242/jcs.127779

Brakebusch, C., Grose, R., Quondamatteo, F., Ramirez, A., Jorcano, J. L., Pirro, A., Svensson, M., Herken, R., Sasaki, T., Timpl, R. et al. (2000). Skin and hair follicle integrity is crucially dependent on beta 1 integrin expression on keratinocytes. *EMBO J.* **19**, 3990-4003. doi:10.1093/emboj/19.15.3990

Conti, F. J. A., Rudling, R. J., Robson, A. and Hodivala-Dilke, K. M. (2003). alpha3beta1-integrin regulates hair follicle but not interfollicular morphogenesis in adult epidermis. *J. Cell Sci.* **116**, 2737-2747. doi:10.1242/jcs.00475

Crew, V. K., Burton, N., Kagan, A., Green, C. A., Levene, C., Flinter, F., Brady, R. L., Daniels, G. and Anstee, D. J. (2004). CD151, the first member of the tetraspanin (TM4) superfamily detected on erythrocytes, is essential for the correct assembly of human basement membranes in kidney and skin. *Blood* **104**, 2217-2223. doi:10.1182/blood-2004-04-1512

Delwel, G. O., de Melker, A. A., Hogervorst, F., Jaspars, L. H., Fles, D. L., Kuikman, I., Lindblom, A., Paulsson, M., Timpl, R. and Sonnenberg, A. (1994). Distinct and overlapping ligand specificities of the alpha 3A beta 1 and

alpha 6A beta 1 integrins: recognition of laminin isoforms. *Mol. Biol. Cell* **5**, 203-215. doi:10.1091/mbc.5.2.203

DiPersio, C. M., Hodivala-Dilke, K. M., Jaenisch, R., Kreidberg, J. A. and Hynes, R. O. (1997). alpha3beta1 Integrin is required for normal development of the epidermal basement membrane. *J. Cell Biol.* **137**, 729-742. doi:10.1083/jcb.137.3.729

Dowling, J., Yu, Q. C. and Fuchs, E. (1996). Beta4 integrin is required for hemidesmosome formation, cell adhesion and cell survival. *J. Cell Biol.* **134**, 559-572. doi:10.1083/jcb.134.2.559

Fontao, L., Dirrig, S., Owaribe, K., Kedinger, M. and Launay, J. F. (1997). Polarized expression of HD1: relationship with the cytoskeleton in cultured human colonic carcinoma cells. *Exp. Cell Res.* **231**, 319-327. doi:10.1006/excr.1996.3465

Geerts, D., Fontao, L., Nievers, M. G., Schaapveld, R. Q. J., Purkis, P. E., Wheeler, G. N., Lane, E. B., Leigh, I. M. and Sonnenberg, A. (1999). Binding of integrin alpha6beta4 to plectin prevents plectin association with F-actin but does not interfere with intermediate filament binding. *J. Cell Biol.* **147**, 417-434. doi:10.1083/jcb.147.2.417

Geuijen, C. A. W. and Sonnenberg, A. (2002). Dynamics of the alpha6beta4 integrin in keratinocytes. *Mol. Biol. Cell* **13**, 3845-3858. doi:10.1091/mbc.02-01-0601

Groves, R. W., Liu, L., Dopping-Hepenstal, P. J., Markus, H. S., Lovell, P. A., Ozoemena, L., Lai-Cheong, J. E., Gawler, J., Owaribe, K., Hashimoto, T. et al. (2010). A homozygous nonsense mutation within the dystonin gene coding for the coiled-coil domain of the epithelial isoform of BPAG1 underlies a new subtype of autosomal recessive epidermolysis bullosa simplex. *J. Invest. Dermatol.* **130**, 1551-1557. doi:10.1038/jid.2010.19

Guo, L., Degenstein, L., Dowling, J., Yu, Q.-C., Wollmann, R., Perman, B. and Fuchs, E. (1995). Gene targeting of BPAG1: abnormalities in mechanical strength and cell migration in stratified epithelia and neurologic degeneration. *Cell* **81**, 233-243. doi:10.1016/0092-8674(95)90333-X

Has, C. and Fischer, J. (2018). Inherited epidermolysis bullosa: new diagnostics and new clinical phenotypes. *Exp. Dermatol.*, doi:10.1111/exd.13668. doi:10.1111/exd.13668

Has, C., Spartà, G., Kiritsi, D., Weibel, L., Moeller, A., Vega-Warner, V., Waters, A., He, Y., Anikster, Y., Esser, P. et al. (2012). Integrin α3 mutations with kidney, lung, and skin disease. *N. Engl. J. Med.* **366**, 1508-1514. doi:10.1056/NEJMoa1110813

Hemler, M. E. (2005). Tetraspanin functions and associated microdomains. *Nat. Rev. Mol. Cell Biol.* **6**, 801-811. doi:10.1038/nrm1736

Jonkman, M. F., de Jong, M. C., Heeres, K., Pas, H. H., van der Meer, J. B., Owaribe, K., Martinez de Velasco, A. M., Niessen, C. M. and Sonnenberg, A. (1995). 180-kD bullous pemphigoid antigen (BP180) is deficient in generalized atrophic benign epidermolysis bullosa. *J. Clin. Invest.* **95**, 1345-1352. doi:10.1172/JCI117785

Kagan, A., Feld, S., Chemke, J. and Bar-Khayim, Y. (1988). Occurrence of hereditary nephritis, pretibial epidermolysis bullosa and beta-thalassemia minor in two siblings with end-stage renal disease. *Nephron* **49**, 331-332. doi:10.1159/000185086

Koster, J., Geerts, D., Favre, B., Borradori, L. and Sonnenberg, A. (2003). Analysis of the interactions between BP180, BP230, plectin and the integrin alpha6beta4 important for hemidesmosome assembly. *J. Cell Sci.* **116**, 387-399. doi:10.1242/jcs.00241

Litjens, S. H. M., de Pereda, J. M. and Sonnenberg, A. (2006). Current insights into the formation and breakdown of hemidesmosomes. *Trends Cell Biol.* **16**, 376-383. doi:10.1016/j.tcb.2006.05.004

Liu, L., Dopping-Hepenstal, P. J., Lovell, P. A., Michael, M., Horn, H., Fong, K., Lai-Cheong, J. E., Mellerio, J. E., Parsons, M. and McGrath, J. A. (2012). Autosomal recessive epidermolysis bullosa simplex due to loss of BPAG1-e expression. *J. Invest. Dermatol.* **132**, 742-744. doi:10.1038/jid.2011.379

Margadant, C., Raymond, K., Kreft, M., Sachs, N., Janssen, H. and Sonnenberg, A. (2009). Integrin α3β1 inhibits directional migration and wound re-epithelialization in the skin. *J. Cell Sci.* **122**, 278-288. doi:10.1242/jcs.029108

McLean, W. H., Pulkkinen, L., Smith, F. J., Rugg, E. L., Lane, E. B., Bullrich, F., Burgeson, R. E., Amano, S., Hudson, D. L., Owaribe, K. et al. (1996). Loss of plectin causes epidermolysis bullosa with muscular dystrophy: cDNA cloning and genomic organization. *Genes Dev.* **10**, 1724-1735. doi:10.1101/gad.10.14.1724

McMillan, J. R., McGrath, J. A., Tidman, M. J. and Eady, R. A. J. (1998). Hemidesmosomes show abnormal association with the keratin filament network in junctional forms of epidermolysis bullosa. *J. Invest. Dermatol.* **110**, 132-137. doi:10.1046/j.1523-1747.1998.00102.x

Michael, M., Begum, R., Fong, K., Pourreyron, C., South, A. P., McGrath, J. A. and Parsons, M. (2014). BPAG1-e restricts keratinocyte migration through control of adhesion stability. *J. Invest. Dermatol.* **134**, 773-782. doi:10.1038/jid.2013.382

Nakamura, H., Sawamura, D., Goto, M., Nakamura, H., McMillan, J. R., Park, S., Kono, S., Hasegawa, S., Paku, S., Nakamura, T. et al. (2005). Epidermolysis bullosa simplex associated with pyloric atresia is a novel clinical subtype caused by mutations in the plectin gene (PLEC1). *J. Mol. Diagn.* **7**, 28-35. doi:10.1016/S1525-1578(10)60005-0

Niessen, C. M., van der Raaij-Helmer, M. H., Hulsman, E. H., van der Neut, R., Jonkman, M. F. and Sonnenberg, A. (1996). Deficiency of the integrin beta 4 subunit in junctional epidermolysis bullosa with pyloric atresia: consequences for hemidesmosome formation and adhesion properties. *J. Cell Sci.* **109**, 1695-1706.

Nievers, M. G., Kuikman, I., Geerts, D., Leigh, I. M. and Sonnenberg, A. (2000). Formation of hemidesmosome-like structures in the absence of ligand binding by the (alpha)6(beta)4 integrin requires binding of HD1/plectin to the cytoplasmic domain of the (beta)4 integrin subunit. *J. Cell Sci.* **113**, 963-973.

Puklin-Faucher, E. and Sheetz, M. P. (2009). The mechanical integrin cycle. *J. Cell Sci.* **122**, 179-186. doi:10.1242/jcs.042127

Qu, H., Wen, T., Pesch, M. and Aumailley, M. (2012). Partial loss of epithelial phenotype in kindlin-1-deficient keratinocytes. *Am. J. Pathol.* **180**, 1581-1592. doi:10.1016/j.ajpath.2012.01.005

Raghavan, S., Bauer, C., Mundschau, G., Li, Q. and Fuchs, E. (2000). Conditional ablation of beta1 integrin in skin. Severe defects in epidermal proliferation, basement membrane formation, and hair follicle invagination. *J. Cell Biol.* **150**, 1149-1160. doi:10.1083/jcb.150.5.1149

Russell, A. J., Fincher, E. F., Millman, L., Smith, R., Vela, V., Waterman, E. A., Dey, C. N., Guide, S., Weaver, V. M. and Marinkovich, M. P. (2003). Alpha 6 beta 4 integrin regulates keratinocyte chemotaxis through differential GTPase activation and antagonism of alpha 3 beta 1 integrin. *J. Cell Sci.* **116**, 3543-3556. doi:10.1242/jcs.00663

Sachs, N., Kreft, M., van den Bergh Weerman, M. A., Beynon, A. J., Peters, T. A., Weening, J. J. and Sonnenberg, A. (2006). Kidney failure in mice lacking the tetraspanin CD151. *J. Cell Biol.* **175**, 33-39. doi:10.1083/jcb.200603073

Sachs, N., Secades, P., van Hulst, L., Kreft, M., Song, J.-Y. and Sonnenberg, A. (2012). Loss of integrin α3 prevents skin tumor formation by promoting epidermal turnover and depletion of slow-cycling cells. *Proc. Natl. Acad. Sci. USA* **109**, 21468-21473. doi:10.1073/pnas.1204614110

Schaapveld, R. Q., Borradori, L., Geerts, D., van Leusden, M. R., Kuikman, I., Nievers, M. G., Niessen, C. M., Steenbergen, R. D., Snijders, P. J. and Sonnenberg, A. (1998). Hemidesmosome formation is initiated by the beta4 integrin subunit, requires complex formation of beta4 and HD1/plectin, and involves a direct interaction between beta4 and the bullous pemphigoid antigen 180. *J. Cell Biol.* **142**, 271-284. doi:10.1083/jcb.142.1.271

Seltmann, K., Roth, W., Kröger, C., Loschke, F., Lederer, M., Hüttelmaier, S. and Magin, T. M. (2013). Keratins mediate localization of hemidesmosomes and repress cell motility. *J. Invest. Dermatol.* **133**, 181-190. doi:10.1038/jid.2012.256

Sincock, P. M., Mayrhofer, G. and Ashman, L. K. (1997). Localization of the transmembrane 4 superfamily (TM4SF) member PETA-3 (CD151) in normal human tissues: comparison with CD9, CD63, and alpha5beta1 integrin. *J. Histochem. Cytochem.* **45**, 515-525. doi:10.1177/002215549704500404

Sonnenberg, A., Calafat, J., Janssen, H., Daams, H., van der Raaij-Helmer, L. M. H., Falcioni, R., Kennel, S. J., Aplin, J. D., Baker, J., Loizidou, M. et al. (1991). Integrin alpha 6/beta 4 complex is located in hemidesmosomes, suggesting a major role in epidermal cell-basement membrane adhesion. *J. Cell Biol.* **113**, 907-917. doi:10.1083/jcb.113.4.907

Sterk, L. M. T., Geuijen, C. A. W., Oomen, L. C. J. M., Calafat, J., Janssen, H. and Sonnenberg, A. (2000). The tetraspan molecule CD151, a novel constituent of hemidesmosomes, associates with the integrin alpha6beta4 and may regulate the spatial organization of hemidesmosomes. *J. Cell Biol.* **149**, 969-982. doi:10.1083/jcb.149.4.969

Sterk, L. M. T., Geuijen, C. A. W., Berg, J. G. van den, Claessen, N., Weening, J. J. and Sonnenberg, A. (2002). Association of the tetraspanin CD151 with the laminin-binding integrinsα 3β1, α6β1, α6β4 and α7β1 in cells in culture and in vivo. *J. Cell Sci.* **115**, 1161-1173.

Stipp, C. S. (2010). Laminin-binding integrins and their tetraspanin partners as potential antimetastatic targets. *Expert Rev. Mol. Med.* **12**, e3. doi:10.1017/S1462399409001355

Termini, C. M. and Gillette, J. M. (2017). Tetraspanins function as regulators of cellular signaling. *Front Cell Dev. Biol.* **5**, 34. doi:10.3389/fcell.2017.00034

Uematsu, J., Nishizawa, Y., Sonnenberg, A. and Owaribe, K. (1994). Demonstration of type II hemidesmosomes in a mammary gland epithelial cell line, BMGE-H. *J. Biochem.* **115**, 469-476. doi:10.1093/oxfordjournals.jbchem.a124361

Underwood, R. A., Carter, W. G., Usui, M. L. and Olerud, J. E. (2009). Ultrastructural localization of integrin subunits β4 and α3 within the migrating epithelial tongue of in vivo human wounds. *J. Histochem. Cytochem.* **57**, 123-142. doi:10.1369/jhc.2008.952176

Vahidnezhad, H., Youssefian, L., Saeidian, A. H., Mahmoudi, H. R., Touati, A., Abiri, M., Kajbafzadeh, A.-M., Aristodemou, S., Liu, L., McGrath, J. A. et al. (2017). Recessive mutation in tetraspanin CD151 causes Kindler syndrome-like epidermolysis bullosa with multi-systemic manifestations including nephropathy. *Matrix Biol.* **66**, 22-33. doi:10.1016/j.matbio.2017.11.003

van der Neut, R., Krimpenfort, P., Calafat, J., Niessen, C. M. and Sonnenberg, A. (1996). Epithelial detachment due to absence of hemidesmosomes in integrin β4 null mice. *Nat. Genet.* **13**, 366-369. doi:10.1038/ng0796-366

Vidal, F., Aberdam, D., Miquel, C., Christiano, A. M., Pulkkinen, L., Uitto, J., Ortonne, J.-P. and Meneguzzi, G. (1995). Integrin beta 4 mutations associated with junctional epidermolysis bullosa with pyloric atresia. *Nat. Genet.* **10**, 229-234. doi:10.1038/ng0695-229

Walko, G., Castañón, M. J. and Wiche, G. (2015). Molecular architecture and function of the hemidesmosome. *Cell Tissue Res.* **360**, 529-544. doi:10.1007/s00441-015-2216-6

Wright, M. D., Geary, S. M., Fitter, S., Moseley, G. W., Lau, L.-M., Sheng, K.-C., Apostolopoulos, V., Stanley, E. G., Jackson, D. E. and Ashman, L. K. (2004). Characterization of mice lacking the tetraspanin superfamily member CD151. *Mol. Cell Biol.* **24**, 5978-5988. doi:10.1128/MCB.24.13.5978-5988.2004

Yang, X., Claas, C., Kraeft, S.-K., Chen, L. B., Wang, Z., Kreidberg, J. A. and Hemler, M. E. (2002). Palmitoylation of tetraspanin proteins: modulation of CD151 lateral interactions, subcellular distribution, and integrin-dependent cell morphology. *Mol. Biol. Cell* **13**, 767-781. doi:10.1091/mbc.01-05-0275

Yang, X., Kovalenko, O. V., Tang, W., Claas, C., Stipp, C. S. and Hemler, M. E. (2004). Palmitoylation supports assembly and function of integrin-tetraspanin complexes. *J. Cell Biol.* **167**, 1231-1240. doi:10.1083/jcb.200404100

Zhang, X.-P., Puzon-McLaughlin, W., Irie, A., Kovach, N., Prokopishyn, N. L., Laferté, S., Takeuchi, K., Tsuji, T. and Takada, Y. (1999). Alpha 3 beta 1 adhesion to laminin-5 and invasin: critical and differential role of integrin residues clustered at the boundary between alpha 3 N-terminal repeats 2 and 3. *Biochemistry* **38**, 14424-14431. doi:10.1021/bi990323b

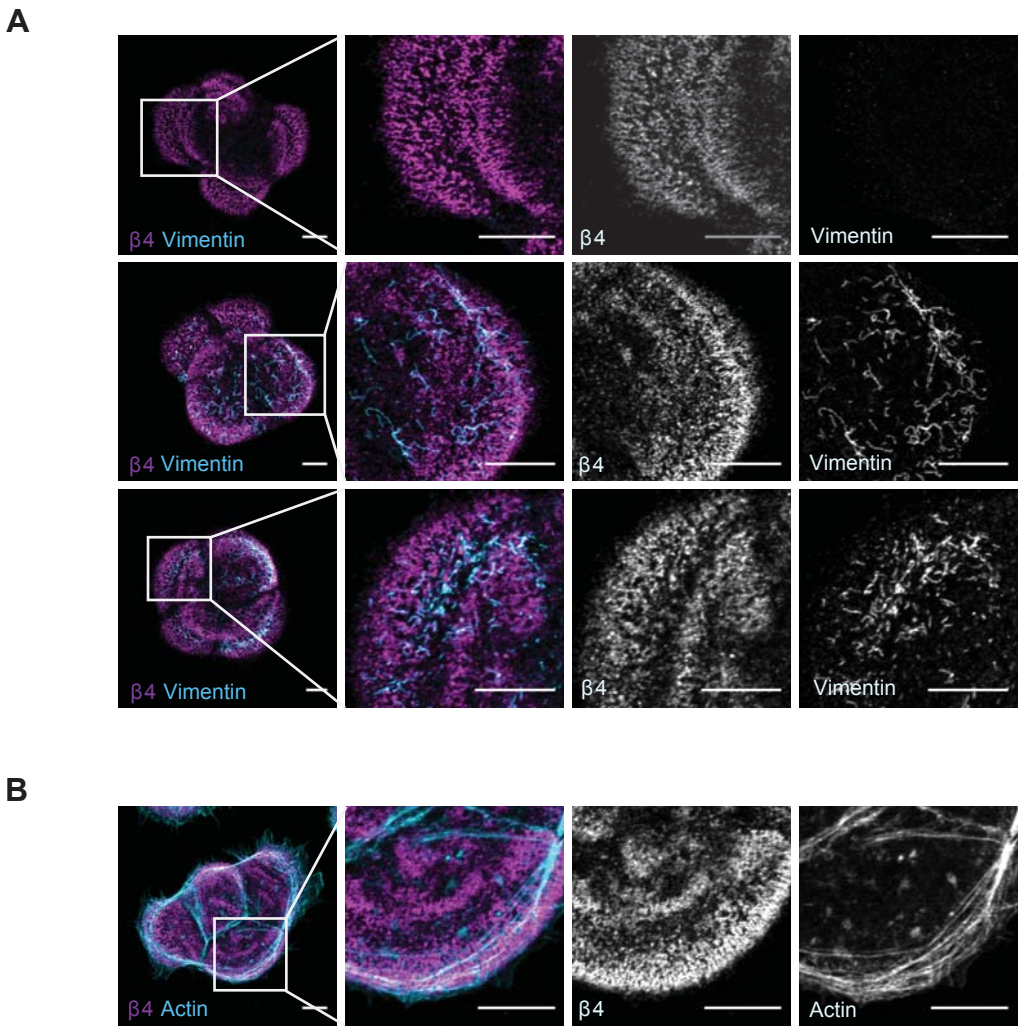

Fig. S1 α6β4 in central HD-like adhesions is not associated with actin or vimentin.
Example overview and zoom-in confocal images of PA-JEB/β4 keratinocytes stained for β4 (magenta) and vimentin (A) or actin (B) (cyan). Top panel of A represents the ~ 50% of PA-JEB/β4 keratinocyt cell islands in which vimentin is absent. Scale bars are 10 µm.

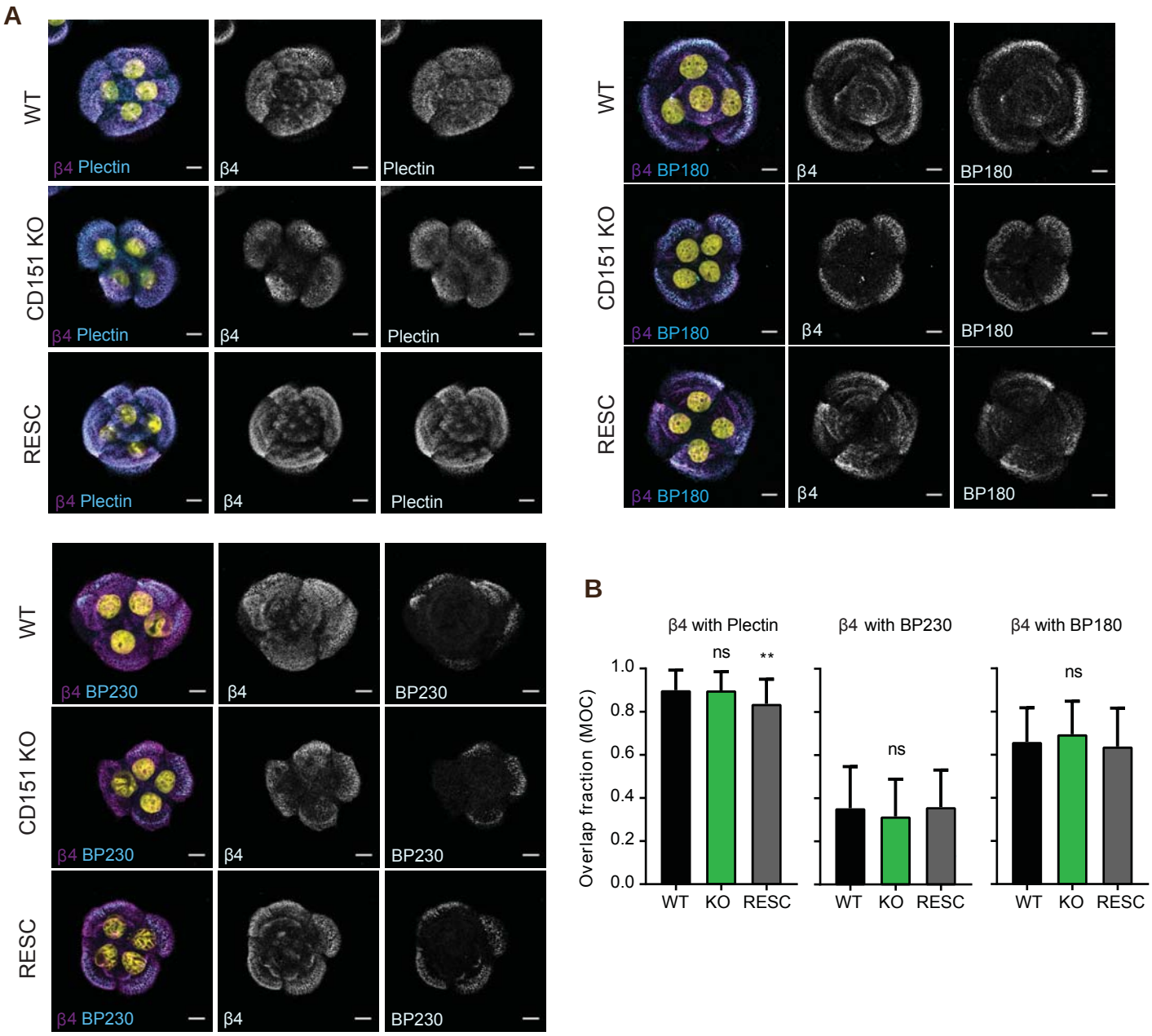

Fig. S2 Type I HDs are formed in the absence of CD151.
(A) Confocal images of WT, CD151-KO and CD151-RESC PA-JEB/β4 keratinocytes stained for plectin, BP180 or BP230 (cyan), β4 (magenta) and DAPI (yellow). Scale bars are 10 µm. B. Quantification of the colocalization (MOC) of β4 with BP180 (WT: 52 images, KO: 47 images, RESC: 48 images; 2 exp. each), BP230 (WT: 97 images, KO: 90 images, RESC: 89 images; 5 exp. each) and plectin (WT: 46 images, KO: 42 images, RESC: 41 images; 3 exp. each) in WT, CD151-KO and CD151-RESC PA-JEB/β4 keratinocytes. Graphs show the mean+s.d.; P value: **< 0.01 (Mann-Whitney U test), ns>0.05.

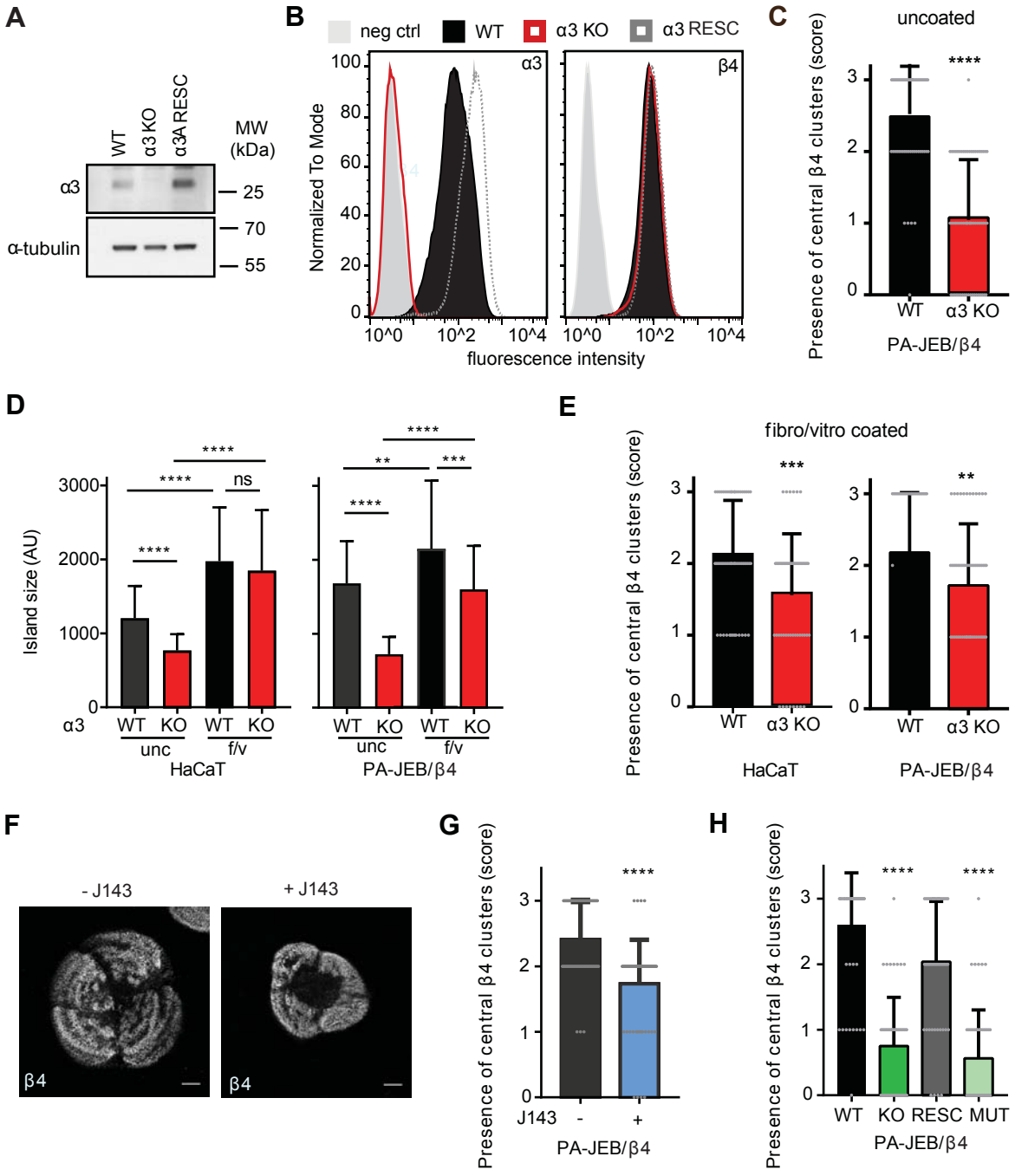

Fig. S3 Confirmation of α3β1 involvement in the maintenance of central HD-like adhesions.
(A) Whole cell lysate of WT, α3-KO and α3-RESC PA-JEB/β4 keratinocytes analyzed by WB for protein levels of α3 and GAPDH (loading control). (B) FACS analyses of α3 and β4 surface expression on WT, α3-KO and α3-RESC PA-JEB/β4 keratinocytes. (C) Quantification of the presence of central β4 clusters (score 0-3) in WT (61 images; 3 exp.) and α3-KO (62 images; 3 exp.) PA-JEB/β4 keratinocytes. (D) Island size of WT and α3-KO HaCaT and PA-JEB/β4 keratinocytes seeded on uncoated (unc) or fibronectin and vitronectin (f/v) coated coverslips (~60 images each; 3 exp.). (E) Quantification of the presence of central β4 clusters (score 0-3) in WT (60 images; 3 exp.) and α3-KO (59 images; 3 exp.) HaCaT keratinocytes, and WT (60 images; 3 exp.) and α3-KO (61 images; 3 exp.) PA-JEB/β4 keratinocytes seeded on fibronectin and vitronectin coated coverslips. (F) Confocal images of β4 in PA-JEB/β4 cells grown on coverslips for two days in the absence (-) or presence (+) of α3 blocking antibody J143. Scale bars are 10 µm. (G) Quantification of the presence of central β4 clusters (score 0-3) in WT PA-JEB/β4 cells grown in the absence (65 images; 3 exp.) or presence (66 images; 3 exp.) of J143. (H) Quantification of the presence of central β4 clusters (score 0-3) in WT (57 images; 4 exp), CD151-KO (56 images; 4 exp.), RESC (55 images; 4 exp.) and MUT (55 images; 4 exp.) PA-JEB/β4 keratinocytes. WT, KO and RESC data is identical to the data depicted in Fig. 2G. Graphs in C, D, E, G and H show the mean+s.d.; P values: **<0.01, ***< 0.001, ****< 0.0001 (Mann-Whitney U test).

Target	Antibody	Application	Source/kind gift from
α-tubulin	Mouse mAb	WB (1:10000)	Sigma-Aldrich #t5168
BP230	5E, human mAb	IF (1:400)	Takashi Hashimoto, Keio University School of Medicine, Shinjuku, Tokyo, Japan
Coll. XVII	VK14, mouse mAb	IF (1:5)	Hendri Pas University Medical Center Groningen, Groningen, The Netherlands
CD151	5C11, mouse mAb	IF (1:1), IP (1:5), WB (1:50)	Fedor Berditchevski University of Birmingham, Birmingham, United Kingdom
CD151	11G5 (IgG1), mouse mAb	IP (1 µg ml^{-1}), FACS (1:400), WB (1:2000)	Jonathan Humphries University of Manchester, Manchester, United Kingdom
CD151	11B1.G4 (p48), mouse mAb	WB (1:2500)	Leonie Ashman University of Newcastle, Newcastle, NSW, Australia.
GAPDH	Rabbit pAb	WB (1:2000)	Cell Signaling #5174
GFP	B34, mouse mAb	WB (1:5000)	Covance
Itg. α3	J143, mouse mAb	IF (1:250), IP (1 µg ml^{-1}), FACS (1:400), blocking (30 µg ml^{-1})	American Type Culture Collection
Itg. α3	A-3, mouse (IgG2a) mAb	IF (1:100)	Santa Cruz #sc-374242
Itg. α3A	Rabbit pAb	WB (1:1000)	In-house
Itg. α6	AA6NT, rabbit pAb	WB (1:500)	Anne Cress University of Arizona, Tucson, Arizona, USA
Itg. α6	GoH3, rat mAb	IP (1 µg ml^{-1})	In-house
Itg. β1	Rabbit pAb	WB (1:2000)	Reinhard Fässler Max Planck Institute of Biochemistry, Martinsried, Germany
Itg. β4	439-9B, rat mAb	IF (1:200)	BD Bioscience #555719
Itg. β4	PE-rat anti-human-CD104	FACS (1:400)	BD Pharmingen #555720
Itg. β4	ASC8, mouse, mAb	Blocking (1:5)	Amy Skubitz University of Minnesota, Minneapolis, MN, USA
Itg. β4	Rabbit pAb	WB (1:2000)	In-house
Keratin 14	Rabbit pAb	IF (1:1000)	Covance #PRB-155P
Laminin-332	R14, rabbit pAb	IF (1:500)	Monique Aumailley University of Cologne, Cologne, Germany
pPaxillin Y31	Rabbit pAb	IF (1:200)	Biosource #44-720G
Plectin	P2, guinea pig pAb	IF (1:400)	Harald Herrmann German Cancer Research Center, Heidelberg, Germany

Table S1. Primary antibodies used in various techniques
Abbreviations used: Immune fluorescence (IF), Immune precipitation (IP), fluorescence-activated cell sorting (FACS) and Western blot (WB).

Movie 1
Movies of a time-lapse experiment using WT (movie S1) and CD151-KO (movie S2) PA-JEB/β4-GFP keratinocytes. Images were taken every hour for 20h, starting from the addition of DMEM+FCS (0h timepoint, 20h after seeding).

Movie 2
Movies of a time-lapse experiment using WT (movie S1) and CD151-KO (movie S2) PA-JEB/β4-GFP keratinocytes. Images were taken every hour for 20h, starting from the addition of DMEM+FCS (0h timepoint, 20h after seeding).

Journal of Cell Science • Supplementary information